BNL High Pressure Program including NSLS II at XPD and 'dark period' APS program at 6BM

Donald J Weidner
Lars Ehm
Michael T Vaughan

BNL High Pressure Program including NSLS II at XPD and 'dark period' APS program at 6BM

2015 COMPRES Annual Report
November 2014 – October 2015
Prepared by Donald Weidner and Lars Ehm

Overview

The program at Brookhaven National Laboratories Light Sources has been in transition during the reporting period of November 2014 to October 2015. The National Synchrotron Light Source ended its operation on September 30. 2014. The closing of the facility followed a five month decommissioning period. We successfully decommissioned the X17 endstations and support laboratory at the end of March 2015 and vacated the National Synchrotron Light Source.

The main focus during the reporting period was the establishment of the high pressure program at the X-ray powder diffraction beamline (XPD) at the National Synchrotron Light Source II. The new facility will be located in hutch D of the XPD beamline and provide X-ray diffraction and imaging capabilities for both Large Volume Press and Diamond Anvil Cell experiments. We estimate a start of the commissioning of the high pressure program at XPD-D in summer of 2015 and a full user operation starting in November 2016.

We also established a 'dark period' high pressure facility at the Advanced Light Source at Argonne National Laboratory. This facility supports a DDIA apparatus with a sample preparation laboratory. Equipment from X17 together with additional Stony Brook equipment was configured and installed to provide an equivalent high pressure facility as the one that operated at X17B2. The system was installed by June, 2015 and has been in operation since. Some equipment problems surfaced and have been fixed. The support laboratory is not entirely finished, but we are accepting outside users and have been having successful experiments.

Scientific Highlights

Although no experiments have been conducted at NSLS or NSLS II in the reporting period, data collected in the past operation cycles at NSLS have been published in the reporting period. Below a number of publications we like to highlight:

Karato Group: The most important achievement during the last ~2 years in my lab is the large strain (~100 %) deformation experiments of lower mantle mineral assembly under the lower mantle conditions (P to 28 GPa, T to 2200 K). These experiments showed that bridgmanite is substantially weaker than (Mg,Fe)O and strain weakening is observed at ~30-40 % strain.

P-V-T equation of state and high-pressure behavior of $CaCO_3$ aragonite

Ying Li[1, 2], Yongtao Zou[1], Ting Chen[3], Xuebing Wang[3], Xintong Qi[3], Haiyan Chen[1], Jianguo Du[2], Baosheng Li[1]

[1] *Mineral Physics Institute, Stony Brook University, Stony Brook, NY 11794-2100, USA*
[2]*CEA Key Laboratory of Earthquake Prediction (Institute of Earthquake Science), China Earthquake Administration, Beijing, 100036, China*
[3]*Department of Geosciences, Stony Brook University, Stony Brook, NY 11794-2100, USA*

The equation of state of aragonite was determined by *in situ* synchrotron X-ray diffraction experiments on a hot-pressed polycrystalline specimen of aragonite within its stability field up to 5.8 GPa and 1173 K. As a complement to this experimental study, first principles density functional theory calculations were performed up to 20 GPa at 0 K. Thermoelastic parameters for aragonite ($CaCO_3$) were derived by a least-squares fit of the experimental P-V-T data to the third-order Birch-Murnaghan equation of state (EOS), yielding the bulk modulus and its pressure and temperature derivatives $K_0 = 65.24 \pm 0.24$ GPa, $K_0' = 4.95 \pm 0.12$, $(\partial K_T/\partial_T)_P = -0.024 \pm 0.002$ GPa K^{-1} and volume thermal expansion $\alpha_{300} = (6.1 \pm 0.7)\times10^{-5}$ K^{-1}. The analyses of the axial compressibility at ambient temperature show that the *c*- axis is much more compressible than the *a*- and *b*- axes. Based on first principles calculations, the anisotropic compression behavior of aragonite structure is explained by the heterogeneous shortening of <Ca-O> and <C-O> bond lengths and the rotation of <O-C-O> angles along the *a*-, *b*-, and *c*-axes, whereas the unit cell volume change of aragonite under compression is accommodated by comparable compression rate of the CaO_9 polyhedra and the voids in the crystal lattice. The results attained from this study provide important thermoelastic parameters for understanding the thermodynamic behavior and chemical reactions involving aragonite at subduction zone conditions.

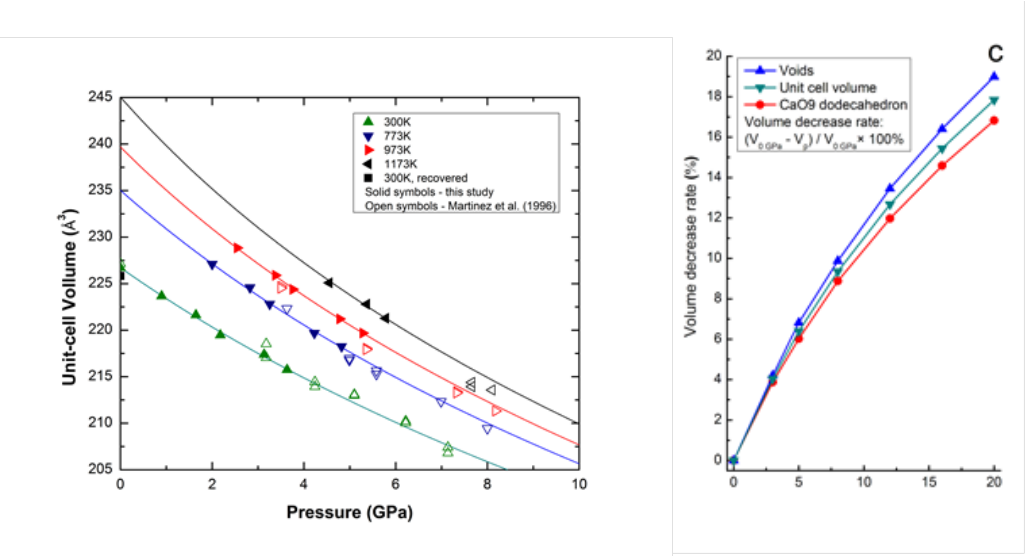

Li, U., Y. Zou, T. Chen, X. Wang, X. Qi, H. Chen, J. Du and B. Li, P-V-T equation of state and high-pressure behavior of CaCO3 aragonite, American Mineralogist, Volume 100, pages 2323–2329, 2015.

Hexagonal-structured ε-NbN: ultra-incompressibility, high shear rigidity, and a possible hard superconducting material

Zou, Y[1,4]., X. Qi[2], X. Wnag[2], T. Chen[2], B. Liu[4], T. Cui[4], B. Li[1],
[1] Mineral Physics Institute, State University of New York, Stony Brook, New York 11794, USA

[2] Department of Materials Science and Engineering, State University of New York, Stony Brook, New York 11794, USA
[3] Department of Geosciences, State University of New York, Stony Brook, New York 11794, USA
[4] Key Laboratory of Functional Materials Physics and Chemistry of the Ministry of Education, Jilin Normal University, Siping 136000, China

Exploring the structural stability and elasticity of hexagonal ε-NbN helps discover correlations among its physical properties for scientific and technological applications. Here, for the first time, we measured the ultra-incompressibility and high shear rigidity of polycrystalline hexagonal ε-NbN using ultrasonic interferometry and in situ X-ray diffraction, complemented with first-principles density-functional theory calculations up to 30 GPa in pressure. Using a finite strain equation of state approach, the elastic bulk and shear moduli, as well as their pressure dependences are derived from the measured velocities and densities, yielding B_{S0} = 373.3(15) GPa, G_0 = 200.5(8) GPa, $\partial B_S/\partial P$ = 3.81(3) and $\partial G/\partial P$ = 1.67(1). The hexagonal ε-NbN possesses a very high bulk modulus, rivaling that of superhard material cBN (B_0 = 381.1 GPa). The high shear rigidity is comparable to that for superhard γ-B (G_0 = 227.2 GPa). We found that the crystal structure of transition-metal nitrides and the outmost electrons of the corresponding metals may dominate their pressure dependences in bulk and shear moduli. In addition, the elastic moduli, Vickers hardness, Debye temperature, melting temperature and a possible superconductivity of hexagonal ε-NbN all increase with pressures, suggesting its exceptional suitability for applications under extreme conditions.

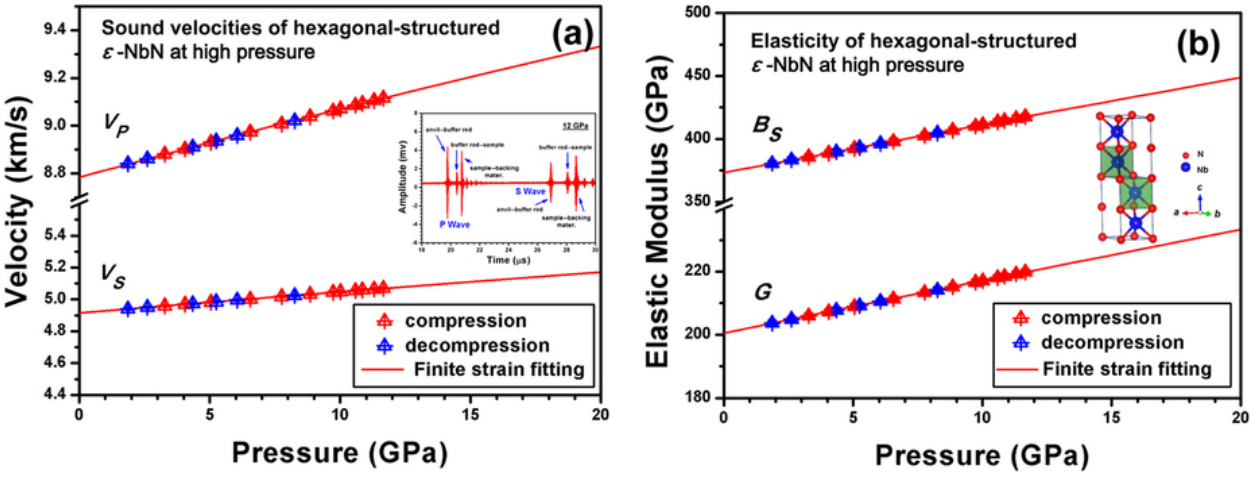

Zou, Y., X. Qi, X. Wnag, T. Chen, B. Liu, T. Cui, B. Li, Hexagonal-structured ε-NbN: ultra-incompressibility, high shear rigidity, and a possible hard superconducting material, Scientific Reports. 06/2015; 5:10811. DOI: 10.1038/srep10811

High-pressure behavior and thermoelastic properties of niobium studied by in situ x-ray diffraction

Yongtao Zou[1], Xintong Qi[2], Xuebing Wang[3], Ting Chen[3], Xuefei Li[1,4], David Welch[2,5] and Baosheng Li[1]

[1] Mineral Physics Institute, State University of New York, Stony Brook, New York 11794, USA
[2] Department of Materials Science and Engineering, State University of New York, Stony Brook, New York 11794, USA
[3] Department of Geosciences, State University of New York, Stony Brook, New York 11794, USA
[4] Key Laboratory of Functional Materials Physics and Chemistry of the Ministry of Education, Jilin Normal University, Siping 136000, China
[5] Condensed Matter Physics and Materials Science Department, Brookhaven National Laboratory, Upton, New York 11973, USA

In situ synchrotron energy dispersive x-ray diffraction (XRD) experiments on Nb have been conducted at pressures up to 6.4 GPa and temperatures up to 1073 K. From the pressure-volume-temperature measurements, thermoelastic parameters were derived for the first time for Nb based on the thermal pressure (ΔPth) equation of state (EOS), modified high-T Birch-Murnaghan EOS, and Mie-Grüneisen-Debye EOS. With the pressure derivative of the bulk modulus fixed at 4.0, we obtained the ambient isothermal bulk modulus K_{T0} = 174(5) GPa, the temperature derivative of bulk modulus at constant pressure GPa K−1 and at constant volume GPa K^{-1}, the volumetric thermal expansivity (K^{-1}), as well as the pressure dependence of thermal expansion K^{-1} GPa^{-1}. Fitting the present data to the Mie-Grüneisen-Debye EOS with Debye temperature Θ_0 = 276.6 K gives γ_0 = 1.27(8) and K_{T0} = 171(3) GPa at a fixed value of q = 3.0. The ambient isothermal bulk modulus and Grüneisen parameter derived from this work are comparable to previously reported values from both experimental and theoretical studies. An in situ high-resolution, angle dispersive XRD study on Nb did not indicate any anomalous behavior related to pressure-induced electronic topological transitions at ~5 GPa as has been reported previously.

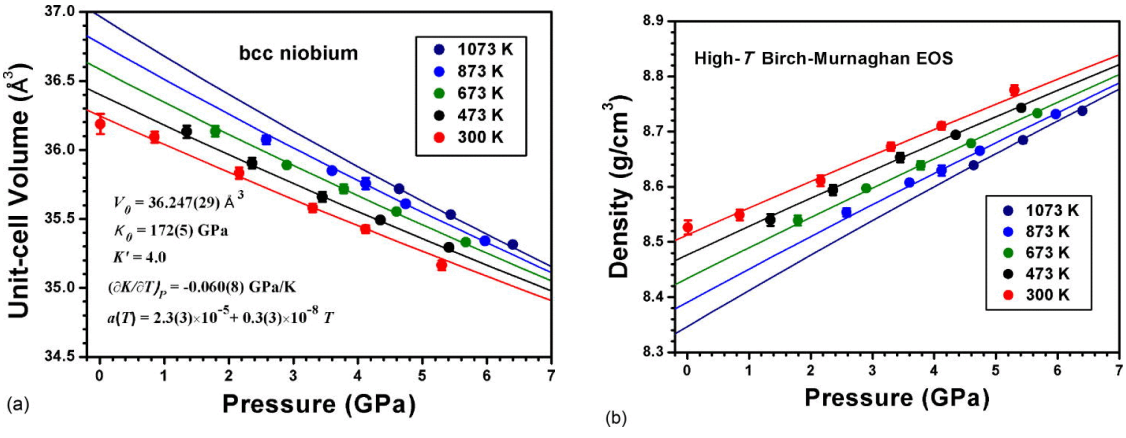

Study of the Earth's interior using measurements of sound velocities in minerals by ultrasonic interferometry

Li, B., R.C. Liebermann (Mineral Physics Institute, Stony Brook University)

This paper reviews the progress of the technology of ultrasonic interferometry from the early 1950s to the present day. During this period of more than 60 years, sound wave velocity measurements have been increased from at pressures less than 1 GPa and temperatures less than 800 K to conditions above 25 GPa and temperatures of 1800 K. This is complimentary to other direct methods to measure sound velocities (such as Brillouin and impulsive stimulated scattering) as well as indirect methods (e.g., resonance ultrasound spectroscopy, static or shock compression, inelastic X-ray scattering). Newly-developed pressure calibration methods and data analysis procedures using a finite strain approach are described and applied to data for the major mantle minerals. The implications for the composition of the Earth's mantle are discussed. The state-of-the-art ultrasonic experiments performed in conjunction with synchrotron X-radiation can provide simultaneous measurements of the elastic bulk and shear moduli and their pressure and temperature derivatives with direct determination of pressure. The current status and outlook/challenges for future experiments are summarized.

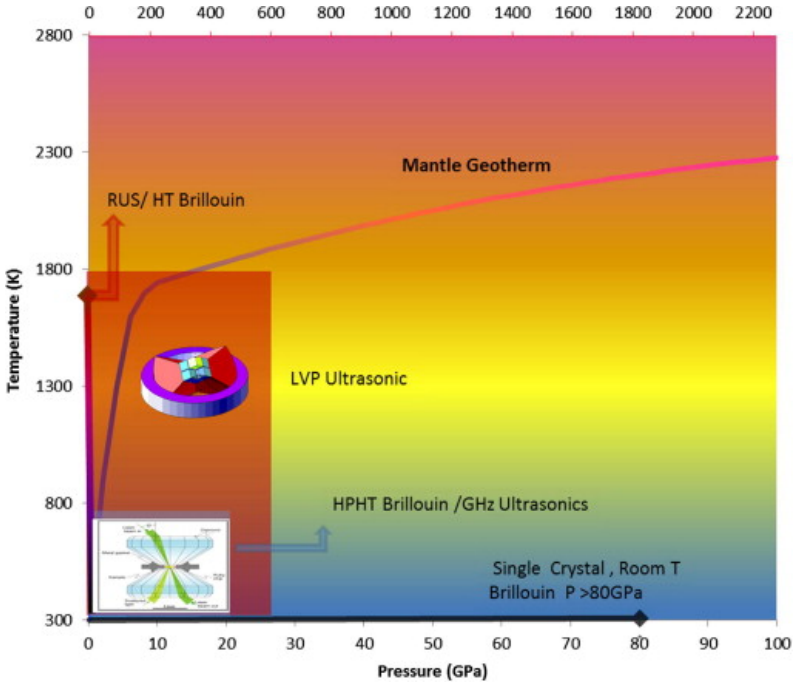

Li, B., and R.C. Liebermann, Study of the Earth's interior using measurements of sound velocities in minerals by ultrasonic interferometry (invited review), Phys. Earth Planet Inter., 233, 135–153, 2014.

Studies of Partial Melting of Peridotite at Mantle Pressures, Temperatures, and Frequencies

Li and Weidner have been exploring the mechanical implications of partial melting using a natural peridotite as the starting material and conducting experiments at the pressure, temperature and frequency as seismic waves in the low velocity zone. Their work, cited in a recent paper by Anderson and King (Driving the Earth machine, 5 December 2014 • VOL 346 ISSUE 6214)

> *In a remarkable series of experiments, Li and Weidner have shown that a solid with pockets of melt oriented by the shearing can produce the kind of low–wave speed, low-viscosity anisotropic material that is consistent with the observed properties of the asthenosphere. Interaction of seismic waves with this material perturbs the material and further reduces the seismic wave speed.*

In their paper, Li and Weidner measure Young's modulus at seismic frequency of a partially molten peridotite as a function of the amount of melt at mantle conditions. They model the effect of partial melting by considering the thermodynamic interaction of the solid and liquid as perturbed by an oscillating stress field. The observations and model are expressed in the following diagrams.

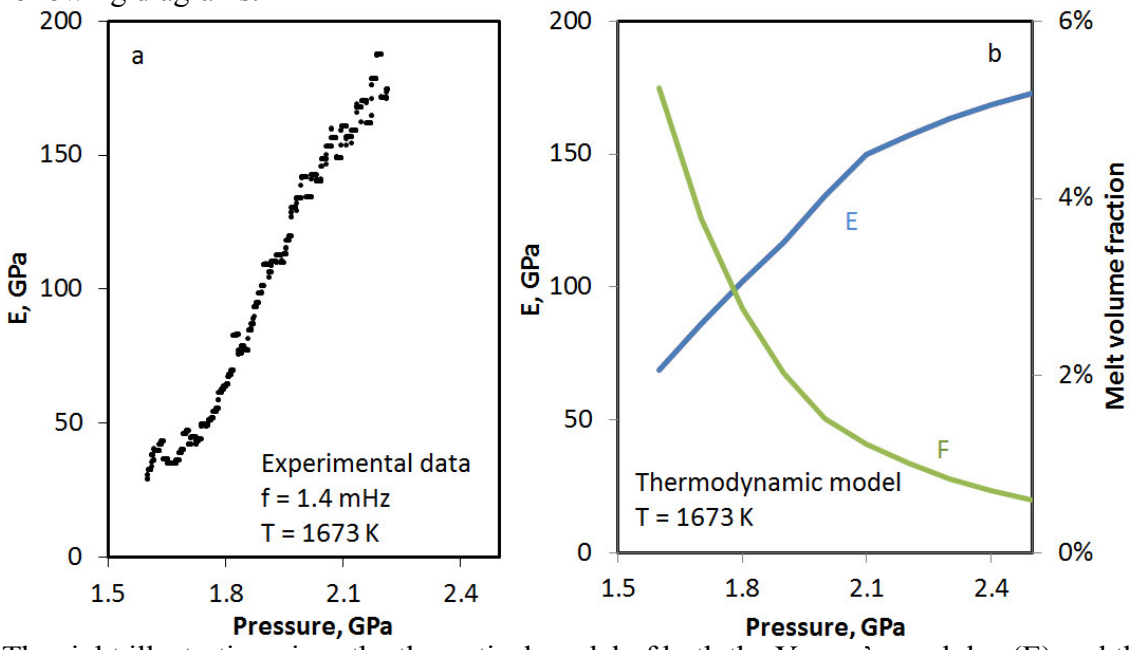

The right illustration gives the theoretical model of both the Young's modulus (E) and the fraction of melt (F). The remarkable result is that the Young's modulus changes by a factor of three in both the data and the model for a change in the four per cent of melt. This effect of melting on the elastic properties has not been considered before.

Reference: Li, L., and D. J. Weidner, Effect of Dynamic Melting on Acoustic Velocities in a Partially Molten Peridotite, Physics of the Earth and Planetary Interior, 222, 1-7, 2013

Kinetics of Partial Melting

Partial melting in the Earth's mantle involves a combination of processes such as ionic diffusion and solid - liquid transition. These processes yield an array of characteristic times for the melting kinetics. Both the magnitude and time constant of melt-induced volume strain affect seismic velocity, attenuation, and buoyancy. In situ monitoring of samples during melting are enabled by multi-anvil high-pressure devices coupled with synchrotron x-ray radiation. In this study, the volume strain induced in a sample from melting is measured as a function of time using x-ray images. We find a doubling of the effective thermal expansion for only 2% melt both from our data and from thermodynamic models of peridotite. The characteristic time of melting is determined to be less than one second. These findings imply that seismic velocities will be sensitive to the strain related to the phase interaction induced by the stress of the seismic wave. The effect is to lower the seismic velocity.

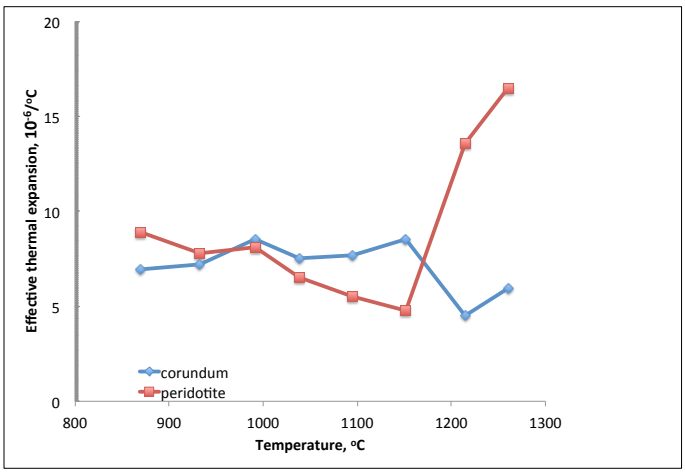

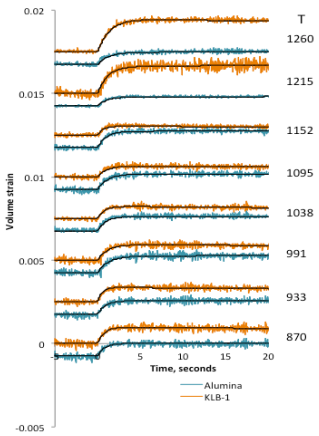

The thermal expansion of the peridotite increased by about a factor of three at the temperature corresponding to the onset of melting. On the right the time dependence of volume is illustrated for several temperatures for both the sample (salmon color) and reference corundum (blue). The rise time of the volume for an instantaneous increase of the furnace temperature reflects the time required for heat to diffuse into the sample. The rise time does not change when melting occurs, indicating that melting is instantaneous compared to the one second rise time. Thus, melting is fast enough to be induced on the 10 – 1000 second time of the seismic stress field.

Reference: Donald J. Weidner and Li Li, Kinetics of melting in peridotite from volume strain measurements, Phys. Earth Planet. Sci., doi:10.1016/j.pepi.2015.06.006

The effect of sintering pressure on anelastictiy of pyrope garnet. (David Dobson, Simon Hunt and Oliver Lord).

Grain-boundary properties affect a diverse range of physical and chemical properties of ceramics, including optical transmission, elastic and viscous properties, partitioning of incompatible elements and electrical conductivity. Despite this, they are a largely neglected aspect of rock- and mineral-physics even though that every rock is a polyscystalline composite (natural ceramic). Here we investigate the effect of sintering pressure on anelasticity of pyrope

garnet.

Garnets were synthesized from $Mg_3Al_2Si_3O_{12}$ glass at 1273 K for 24 h at pressures of between 4 and 15 GPa. The mean grain size was ~2 μm for all samples but those recovered from 15 GPa ware white while those recovered from lower pressures were grey-black. Cored cylinders of pyrope were compressed to 2.5 GPa and subjected to sinusoidally time-varying microstrains in the D-Dial press installed at X17B2 beamline of the NSLS: stress was determined using the length variation of a corundum proxy placed in series with the pyrope sample. The figures below show apparent Young's moduli based on Maxwell viscoelastic fits to the stress-strain data: (A) is for samples annealed at different pressures, all at a driving period of 160s and (B)is for the sample annealed at 4 GPa across a range of driving periods (10-360 s). All samples start off in agreement with the single-crystal average at low temperature and show viscoelastic softening ta the annealing temperature (1273 K) as is common for ceramics. At higher temperatures only the samples sintered at 10 and 15 GPa show significant recovery; the sample sintered 4GPa shows strong dispersion.

The present results show that anelastic behavior is strongly sensitive to sintering pressure, even if the anelasticity measurements are performed under identical conditions. The most likely explanation is that elastically-accommodated grain-boundary sliding is inhibited by strong intergranular bonding at high sintering pressures. This implies that studies which seek to interpret seismic Q values of the lower mantle and inner core (at pressures of 20-360 GPa) on the basis of low-pressure anelasticity measurements are likely to be erroneous.

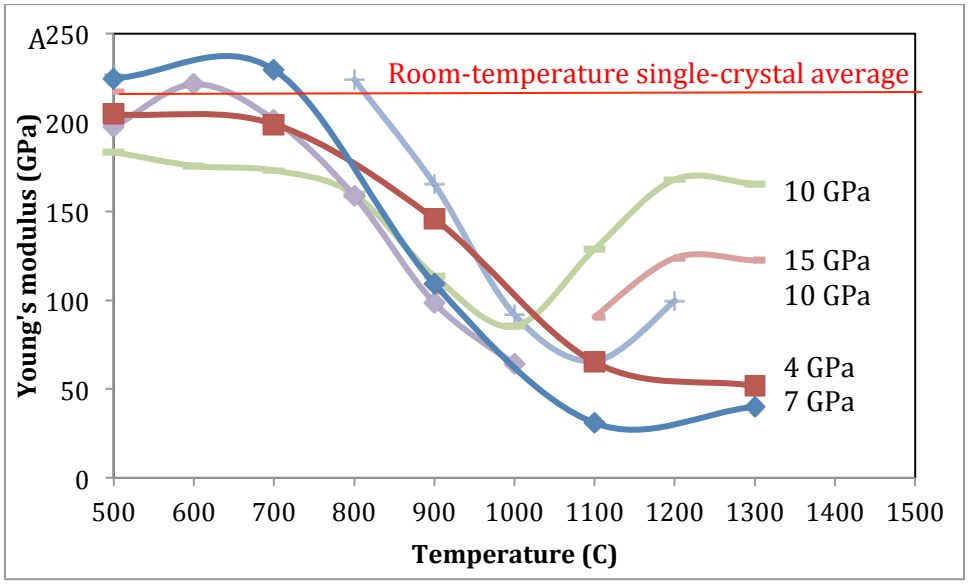

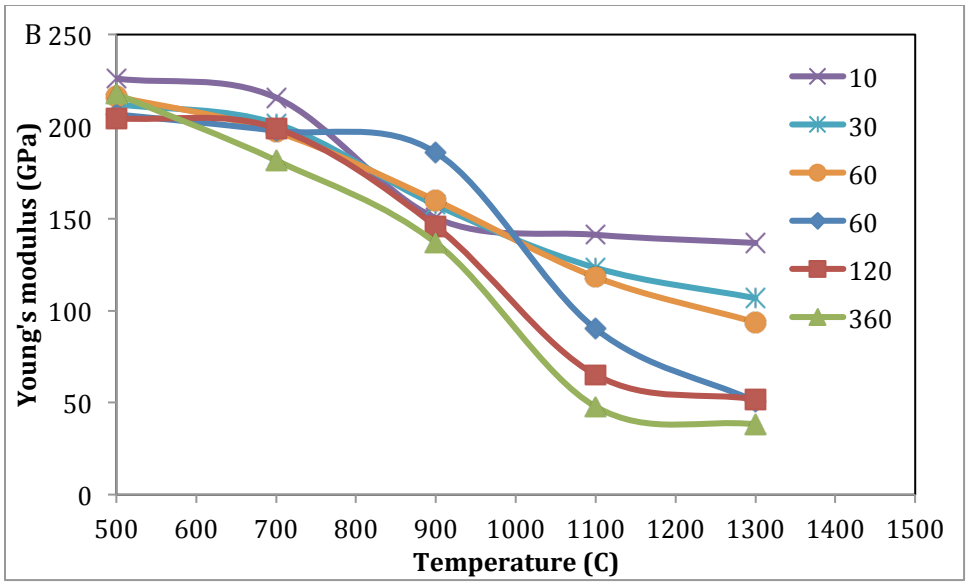

Strength and texture of Pt compressed to 63 GPa

Dorfman et al carried out angle- and energy-dispersive X-ray diffraction experiments in a radial geometry in the diamond anvil cell on polycrystalline platinum samples at pressures up to 63 GPa. It is observed that yield strength and texture depend on grain size. For samples with 70–300-nm particle size, the yield strength is 5–6 GPa at 60 GPa. Coarse-grained (2-lm particles) Pt has a much lower yield strength of 1–1.5 GPa at 60 GPa. Face-centered cubic metals Pt and Au have lower strength to shear modulus ratio than body-centered cubic or hexagonal close-packed metals. While a 300-nm particle sample exhibits the <110> texture expected of face-centered-cubic metals under compression, smaller and larger particles show a weak mixed <110> and <100> texture under compression. Differences in texture development may also occur due to deviations from uniaxial stress under compression in the diamond anvil cell.

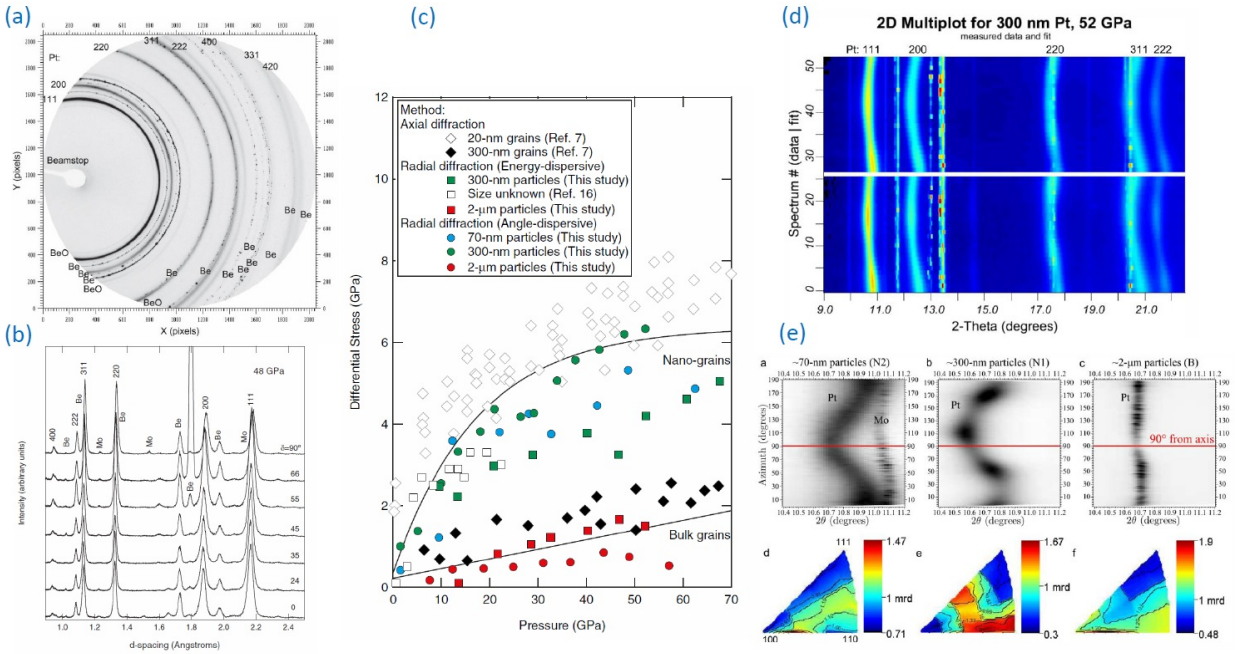

Figure 1. Left panel: (a) Angle-dispersive diffraction pattern for nano-grained Pt sample N1 at 52 GPa; (b) Energy-dispersive diffraction patterns for bulk Pt (sample B) at 48 GPa. **Middle panel**: (c) Maximum differential stress, or yield strength, measured for Pt samples of different grain size. **Right panel:** (d) Full-profile refinement of Pt sample N1 at 52 GPa; (e) Strain and texture in Pt 111 line at 49–52 GPa for samples with different particle sizes

Reference: S.M. Dorfman, S.R. Shieh, T.S. Duffy, Strength and texture of Pt compressed to 63 GPa, Journal of Applied Physics, **117** (2015) 065901.

Maskelynite formation via solid-state transformation: Evidence of infrared and X-ray anisotropy

In this paper, Jaret et al present the results of a combined study of shocked labradorite from the Lonar crater, India, using optical microscopy, micro-Raman spectroscopy, nuclear magnetic resonance (NMR) spectroscopy, high-energy X-ray total scattering experiments, and micro-Fourier transforminfrared (micro-FTIR) spectroscopy. It is found that maskelynite of shock class 2 is structurally more similar to fused glass than to crystalline plagioclase. However, there are slight but significant differences—preservation of original preimpact igneous zoning, anisotropy at infrared wavelengths, X-ray anisotropy, and preservation of some intermediate range order—which are all consistent with a solid-state transformation from plagioclase to maskelynite.

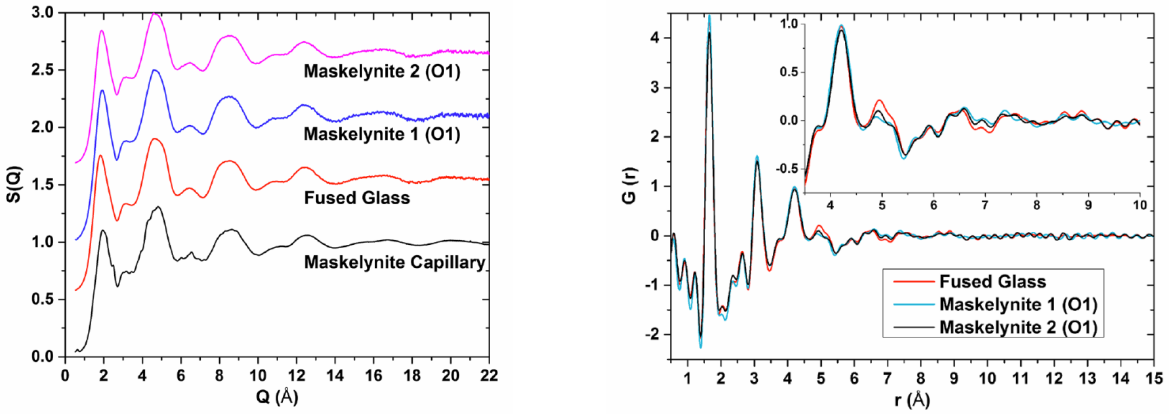

(a) (b)

Figure 1. Left panel: (a) Structure factor S(Q) of four different maskelynite samples—two single maskelynite grains, assorted maskelynite grains in a capillary, and a fused glass with An60 composition. Even despite compositional differences between maskelynite (An63) and the fused glass (An60), the different samples are undistinguishable on the basis of the structure factor. **Right panel:** The pair distribution function G(r) of two different maskelynite grains and fused glass. The inset shows the region characteristic for the intermediate range order in the atomic arrangement.

Reference: S.J. Jaret, W.R. Woerner, B.L. Phillips, L. Ehm, H. Nekvasil, S.P. Wright, T.D. Glotch, Maskelynite formation via solid-state transformation: Evidence of infrared and X-ray anisotropy, Journal of Geophysical Research: Planets, **120** (2015) 570-587.

Dry $(Mg,Fe)SiO_3$ perovskite in the Earth's lower mantle

Combined synthesis experiments and first-principles calculations show that $MgSiO_3$-perovskite with minor Al or Fe does not incorporate significant OH under lower mantle conditions. Perovskite, stishovite, and residual melt were synthesized from natural Bamble enstatite samples (Mg/(Fe + Mg) = 0.89 and 0.93; Al_2O_3 < 0.1 wt % with 35 and 2065 ppm weight H_2O, respectively) in the laser-heated diamond anvil cell at 1600–2000 K and 25–65 GPa. Combined Fourier transform infrared spectroscopy, X-ray diffraction, and ex situ transmission electron microscopy analysis demonstrates little difference in the resulting perovskite as a function of initial water content. Four distinct OH vibrational stretching bands are evident upon cooling below 100 K (3576, 3378, 3274, and 3078 cm^{-1}), suggesting four potential bonding sites for OH in perovskite with a maximum water content of 220 ppm weight H_2O, and likely no more than 10 ppm weight H_2O.

Complementary, Fe-free, first-principles calculations predict multiple potential bonding sites for hydrogen in perovskite, each with significant solution enthalpy (0.2 eV/defect). We calculate that perovskite can dissolve less than 37 ppm weight H_2O (400 ppm H/Si) at the top of the lower mantle, decreasing to 31 ppm weight H_2O (340 ppm H/Si) at 125 GPa and 3000 K in the absence of a melt or fluid phase. We propose that these results resolve a long-standing debate of the perovskite melting curve and explain the order-of-magnitude increase in viscosity from upper to lower mantle.

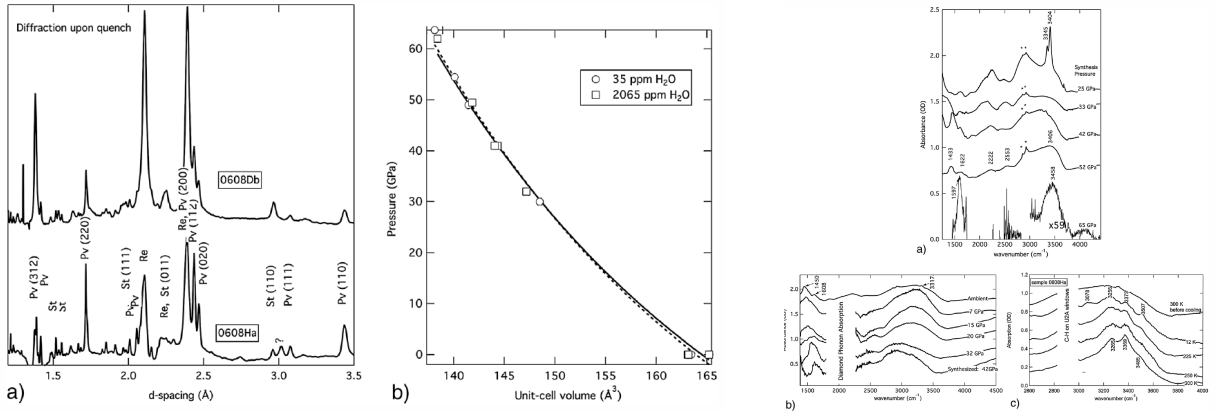

Figure 1. Left panel: X-ray diffraction patterns of experiments 0608Ha (bottom) and 0608Db (top) quenched to ambient pressure. (b) Pressure-volume relationship of perovskite formed from sample 14,516 (circles) and sample 3941 (squares), where uncertainties are less than 20% the size of the symbols. No significant differences in zero-pressure volume or bulk modulus are found to 60 GPa. **Right panel:** (a) Zero-pressure FTIR spectra of perovskite synthesized from 3941 as a function of synthesis pressure; (b) Decompression of sample 0608Ha laser heated at 42 GPa in an argon pressure medium to ambient pressure. (c) FTIR of sample 0608Ha cooled to 12 K at 10^{-6} torr after synthesis and recovery.

Reference: W.R. Panero, J.S. Pigott, D.M. Reaman, J.E. Kabbes, Z. Liu, Dry (Mg,Fe)SiO3 perovskite in the Earth's lower mantle, Journal of Geophysical Research: Solid Earth, 120 (2015) 894-908.

Atomic disorder in $Gd_2Zr_2O_7$ pyrochlore

$Gd_2Zr_2O_7$ pyrochlore with different degrees of cation disorder were synthesized by isothermal annealing at various temperatures (1100–1550C), and the related changes in the structure were investigated by ambient and high pressure x-ray diffraction (XRD) measurements. Unit cell parameters increase almost linearly with increasing treatment temperature. The degree of cation order in pyrochlore also increases with the increase of temperature, but saturates at 60%. The compressibility of the pyrochlore structures decreases when the degree of cation order increases. High pressure XRD measurements also indicate that the phase stability of $Gd_2Zr_2O_7$ is not very sensitive to the degree of atomic disorder in the pyrochlore structure.

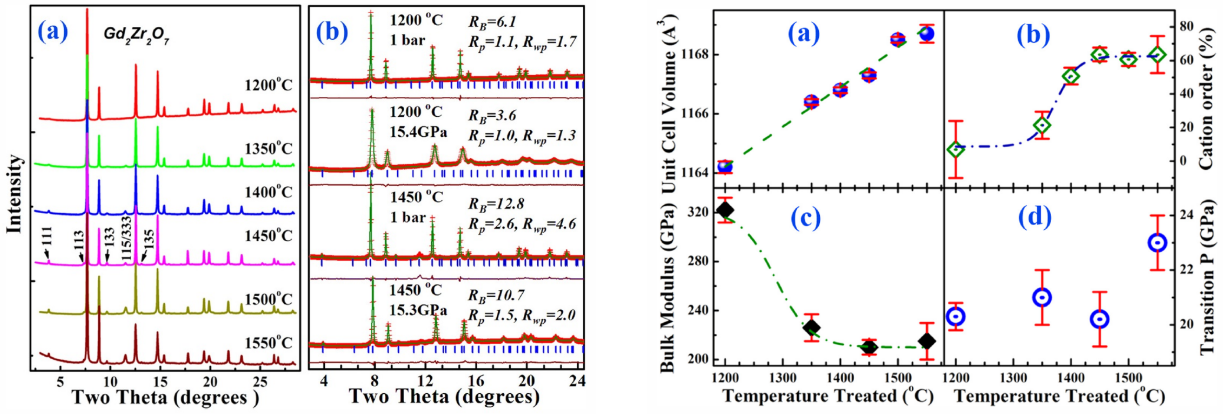

(a) (b)

Figure 1. Left panel: (a) XRD profiles of $Gd_2Zr_2O_7$ pyrochlores treated at different temperatures with various degrees of cation order. The Muller index for the superlattice diffraction maxima is marked on the XRD pattern of the sample treated at 1450ºC. (b) Rietveld refinement results of selected XRD patterns. **Right panel:** Structural properties of $Gd_2Zr_2O_7$ pyrochlores treated at different temperatures. (a) Unit cell volume increases linearly with the treatment temperature; (b) degree of cation order significantly increased in the high temperature samples, but saturates at a maximum of 60%; (c) bulk modulus decreases with increasing degree of cation order; (d) critical transition pressure shows no distinct difference as a function of degree of disorder in the pyrochlore structure-type.

Reference: F.X. Zhang, M. Lang, R.C. Ewing, Atomic disorder in Gd2Zr2O7 pyrochlore, Applied Physics Letters, **106** (2015) 191902.

Pressure-induced stiffness of Au nanoparticles to 71 GPa under quasi-hydrostatic loading

The compressibility of nanocrystalline gold (n-Au, 20 nm) has been studied by X-ray total scattering using high-energy monochromatic X-rays in the diamond anvil cell (DAC) under quasi-hydrostatic conditions up to 71 GPa. The bulk modulus, K_0, of the n-Au obtained from fitting to a Vinet equation of state is ~196(3) GPa, which is about 17% higher than for the corresponding bulk materials (K0: 167 GPa). At low pressures (<7 GPa), the compression behavior of n-Au shows little difference from that of bulk Au. With increasing pressure, the compressive behavior of n-Au gradually deviates from the equation of state (EOS) of bulk gold. Analysis of the pair distribution function (PDF), peak broadening and Rietveld refinement reveals that the microstructure of n-Au is nearly a single-grain/domain at ambient conditions, but undergoes substantial pressure-induced reduction in grain size until 10 GPa. The results indicate that the nature of the internal microstructure in n-Au is associated with the observed EOS difference from bulk Au at high pressure. Full-pattern analysis confirms that significant changes in grain size, stacking faults, grain orientation and texture occur in n-Au at high pressure. We have observed direct experimental evidence of a transition in compression mechanism for n-Au at ~20 GPa, i.e., from deformation dominated by nucleation and motion of lattice dislocations (dislocation-mediated) to a prominent grain boundary mediated response to external pressure. The internal microstructure inside the nanoparticle (nanocrystallinity) plays a critical role for the macro-mechanical properties of nano-Au.

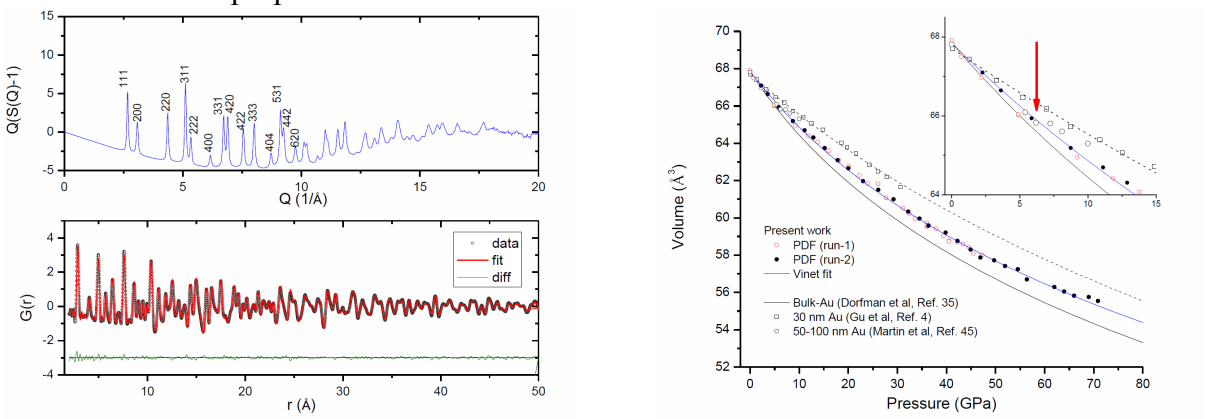

(a) (b)

Figure 1. Left panel: (a) Measured pair distribution function (PDF) of n-Au using high-energy X-ray microbeam (wavelength of 0.15231±0.00004 Å or 81.400±0.024 keV). (Upper panel) Reduced total scattering function F(Q) obtained from the nano Au powder at ambient pressure. (Lower panel) Points are the corresponding PDF function G(r) obtained with an upper limit for the Fourier transform of Q_{max} = 20 $Å^{-1}$. Lines are the simulated PDFs for a structure solution of 22 nm n-Au with a fit residual, R_w, of 0.094. The bottom curve is the difference between measured and simulated PDFs. **Right panel:** Pressure dependence of the unit cell volume of n-Au compared to previously reported data for 300nm Au (dashed line) and the bulk material (solid line). Vinet EOS fit is shown for the PDF data of run-1 and run-2.

Reference: X. Hong, T.S. Duffy, L. Ehm, D.J. Weidner, Pressure-induced stiffness of Au nanoparticles to 71 GPa under quasi-hydrostatic loading, Journal of Physics: Condensed Matter, accepted (in press) (2015).

Some thermodynamic properties of larnite (β-Ca_2SiO_4) constrained by high T/P experiment and/or theoretical simulation

Pure larnite (β-Ca_2SiO_4; Lrn) was synthesized at 6 GPa and 1473 K for 6 hours by using a cubic press, its thermal expansivity was investigated up to 923 K by using an X-ray powder diffraction technique (ambient *P*), and its compressibility was investigated up to ~16 GPa by using a diamond anvil cell coupled with synchrotron X-ray radiation (ambient *T*). Its volumetric thermal expansion coefficient (α_V) and isothermal bulk modulus (K_T) were constrained as α_V = 4.24(4)×10^{-5}/K and K_T = 103(2) GPa (the first pressure derivative K_T' obtained as 5.4(4)), respectively. Its compressibility was further studied with the CASTEP code using density functional theory and planewave pseudopotential technique. We obtained the K_T values as 123(3) GPa (LDA; high boundary) and 92(2) GPa (GGA; low boundary), with the values of the K_T' as 4.4(9) and 4.9(5), respectively. The phonon dispersions and vibrational density of states (VDoS) of Lrn were simulated using density functional perturbation theory, and the VDoS was combined with a quasi-harmonic approximation to compute the isobaric heat capacity (CP) and standard vibrational entropy (S^0_{298}), yielding CP = 212.1(1) – 9.69(5)×$10^2T^{-0.5}$ – 4.1(3)×10^6T^{-2} + 5.20(7)×10^8T^{-3} J mol^{-1} K^{-1} for the *T* range of ~298-1000 K and S^0_{298} =129.8(13) J mol^{-1} K^{-1}. The microscopic and macroscopic thermal Grüneisen parameters of Lrn at 298 K were calculated to be 0.75(6) and 1.80(4), respectively.

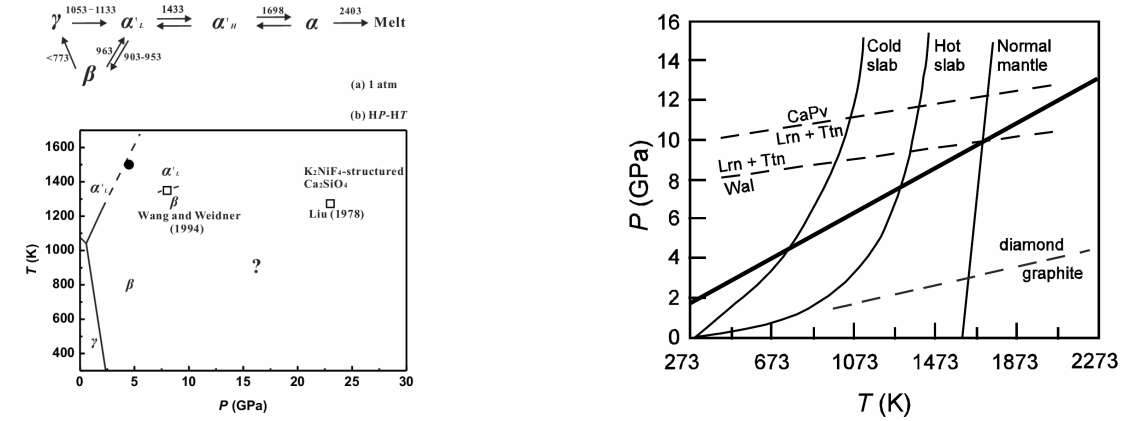

(a) (b)

Figure 1. Left panel: (a) Phase diagram of composition Ca2SiO4. **Right panel:** P-T trajectory for trapping the Lrn inclusion by the diamonds from the Kankan district of Guinea (thick curve). The *P*-*T* profiles of the cold slab and hot slab are sketched from Thompson (1992), and the *P*-*T* profile for the normal mantle follows the 1600 K adiabat for the simplified pyrolite composition in Jackson (1998). Since the Lrn inclusion always coexists with the Ttn phase (Joswig et al. 1999), the phase boundaries between Wal and Lrn + Ttn (equation 1), and between Lrn + Ttn and CaPv (equation 2) are plotted to show the stability field of the phase assemblage Lrn + Ttn (Gasparik et al. 1994; Sueda et al. 2006). The well known phase boundary of graphite and diamond is also sketched.

Reference: Z. Xiong, X. Liu, S.R. Shieh, S. Wang, L. Chang, J. Tang, X. Hong, Z. Zhang, H. Wang, Some thermodynamic properties of larnite (β-Ca_2SiO_4) constrained by high T/P

experiment and/or theoretical simulation, American Mineralogist (accepted, in press) (2015).

N_{Ge}^{O} *Beamline Personnel*

Operation is located at two synchrotron sources, the Advanced Photon Source at Argonne National Laboratory and the National Synchrotron Light Source II at Brookhaven National Laboratory.

The project leadership is comprised of Donald Weidner, Michael Vaughan and Lars Ehm. The operation and the personal support are heavily leveraged by staff of the Mineral Physics Institute at Stony Brook University and Facility Staff at Brookhaven National Laboratory and at Argonne National Laboratory.

The subcontract from COMPRES supported: Matthew Whitaker (LVP XPD-D), Haiyen Chen (LVP 6 BM), Xinguo Hong (DAC XPD-D), William Huebsch (Electronic Support XPD & 6 BM)

Additionally, the operation is supported by the following staff members of the Mineral Physics Institute at Stony Brook University: Kenneth Baldwin (Software/Controls Specialist), Samantha Lin (Administrative Support); Lars Ehm; Michael Vaughan; and Donald Weidner

Establishing the high pressure program at XPD-D at the NSLS II is supported by a significant number of NSLS II staff: Eric Dooryhee (XPD Lead Scientist), Sanjit Ghoose (XPD Scientist), Hengzi Wang (XPD Engineer), John Trunk (XPD Technician), Chris Stebbins (Safety Engineer), Wayne Lewis (Controls Group), Lars Ehm (SBU/BNL Joint Appointee)

Beamline Operations

Brookhaven National Laboratory

The main activities of the Brookhaven centered high pressure program during the reporting period was the transition of the NSLS user program to the NSLS-II. The previously developed decommission plan was executed and the three experimental endstations X17B2, X17B3 and X17C were fully decommissioned.

Decommissioning of the X17B3 endstation: Start of the effort is shown on the right (October 5. 2014) and the final stages of the decommissioning effort on the left (February 15. 2015).

The program vacated the X17 area at the NSLS on March 30. 2015. Main parts of the X17B2 and X17B3 equipment have already been transferred to NSLS II to build the foundation for the high pressure program at XPD-D. The remaining equipment was transported to Stony Brook University for storage until the installation process at XPD-D starts. The significant amount of work performed by our beamline staff in close collaboration with the NSLS decommissioning and stabilization team is documented in the included photos.

Finished decommissioning of X17C hutch (left) and support laboratory (right) at NSLS.

Parallel to the decommissioning efforts we started to develop a comprehensive installation and safety plan in close collaboration with the facility staff at NSLS II. As one of the first Partner User Programs at a project beamline on the NSLS II floor, that installs its own hardware, the installation process is under additional scrutiny.

The installation plan is comprised of:

1. Installation Plan
    a. Task break down
    b. Hazard analysis
    c. 3D CAD Model of the equipment in hutch D
    d. Work planning

2. Safety Plan

a. Complete ray tracing of beam path for radiation safety
b. Laser safety review
    i. Interlocks and engineering controls
    ii. Administrative controls
c. Press and hydraulics review
    i. Interlocks and engineering controls
    ii. Administrative controls
d. Safety Documentation

3. Motion Control upgrade
    a. Identification of all motors (incl. parameters) on DAC and LVP setup
    b. Identification of DeltaTau controller modules
    c. Replacement plan for incompatible motors
    d. Migration plan to NSLS II control environment
    e. Integration into NSLS II data acquisition and data management structure

We have started to execute the first steps of the installation plan. The experimental base for the diamond anvil cell program and the large volume press has been positioned in the XPD-D hutch. We coordinating closely with NSLS staff and BNL service group the individual tasks that need to be performed by COMPRES-MPI staff and/or BNL service groups.

We anticipate the installation efforts be completed in summer 2016 followed by an Instrument Readiness Review (IRR) by the NSLS II facility. After the IRR we will start the commissioning of Commissioning of the high pressure program. We will start to develop the detailed commissioning plan for the high pressure program at XPD-D early 2016. As of today, we expect the start of user aided commissioning after September 2016 and the start of the official user program in the first cycle of 2017.

Argonne National Laboratory

Activities have included disassembling The X17B2 facility, extracting a workable system supplemented by Stony Brook equipment, assembling the electronics and hydraulics at Stony Brook to assure a working system, shipping all to APS, reassemble all parts and getting it working. This process took from October, 2014 to June, 2015. We are now finalizing the user support laboratory and are open for business. We clearly suffer from a weaker beam than we had at X17, but it is sufficient for most experiments.

Performance Metrics

See Attached Excel file

Beamline Community Activities

Xinguo Hong presented instrument developments and research at two international conferences, the 12th Synchrotron Radiation Instrumentation (SRI) conference and the 23rd International Congress on X-ray Optics and Microanalytics (ICXOM23) during 2015.

The titles of the presentations were:
High-pressure Pair Distribution Function (PDF) Measurement in the Diamond Anvil Cell using High-energy Focused X-ray Beam, X.Hong, L. Ehm, T.S. Duffy, D.J. Weidner and S. Ghose (SRI)

High-energy X-ray focused microbeam by using KB mirrors and sagittal bent Laue monochromator, X. Hong (IXCOM)

Furthermore, Xinguo Hong's research leads to a number of accepted peer-reviewed publications in the reporting period. The publications are included in the appended list of publications.

Don Weidner has become the vice chair of the User Executive Committee. This position will become chair next year. I currently meet monthly with the Director of the NSLS II and with the Associate Lab Director for facilities.

Beamline Development

While the beamline development at NSLS II is on hold, we focused on further development and commissioning of the pressure and temperature generating devices. The laser heating system was installed at Stony Brook University and we continued the development and implementation of the temperature measurement system. We successfully commissioned the temperature measurement system and are currently optimizing out system prior to the installation at XPD-D in spring 2016

As outlined above, the APS program has been set up and is operational.

Planned Activities

Planning an Earth Science Village Workshop at the annual NSLS-II\CFN user meeting in May 2016. See appendix for a description of current vision for the village.

"Beamline" Development proposal for the Earth Science Village across a number of established and new beamlines. In response to the call for beamline proposals after the strategic planning meeting, we are planning a proposal that will provide NSLS II certification to a Earth Science Village. This will involve a number of existing and planned beamlines. We now have a small 'brain storming' group that is working to identify new high pressure facilities that need to be developed to take advantage of the HEX beamline that includes traditional mineral physics high pressure along with rock mechanics type science.

Our view is that the next few years will be a building time, starting with XPD, then

including *in situ* inelastic scattering (IXS), *in situ* microprobe studies (SRX), large scale imaging (HEX), and infra red (FIS). These would be supplemented with *ex situ* studies at the tender x-ray beamline TES as well as the Center for Nanno Materials (CFN). The list of beamlines that will be included in the village will expand with time as the capabilities of these beamlines are integrated into the Earth Science Toolbox. Staff time will be spent between user support, beamline development, and scientific expansion of beamline capabilities. Over the next five years we expect a significant fraction of resources devoted to the development aspect.

Budget

Expenditures so far this year

	NSLS/NSLS II	APS
BL scientist /DAC	$31,403	
BL scientist/MAC	$943	$30,690
BL scientist/MAC	$30,770	
Technical Specialist/ MAC	$9,923	
Fringe Benefits (.41)	$31,907	$13,424
Summer Support	$1,899	
Summer Support Fringe	$494	
Equipment*		
Travel	$20,894	$17,979
Supplies	$10,942	$4,588
Services	$3,804	$4,368
Shop support	$528	
Moving		
subtotal direct costs	$143,506	$71,049
IDC (.26) - not equipment	$37,312	$18,473
Totals	$180,817	$89,522
Grand total	$270,339	

The rate of expenditure this year has been delayed by decommissioning and moving. We

will replenish our inventories and fill out our support laboratory during the rest of the year.

Budget for 2016-2017

	APS	NSLS II	sum
Technical officer/DAC BL, Hong		$83,850.00	$83,850.00
BL scientist/MAC, Chen	$83,850.00		$83,850.00
BL scientist/MAC, Whitaker		$83,850.00	$83,850.00
Electronics, Heubsch		$25,000.00	$25,000.00
Fringe Benefits (.45)	$37,732.50	$86,715.00	$124,447.50
Equipment	$0.00	$0.00	$0.00
Travel	$13,600.00	$7,200.00	$20,800.00
Supplies	$30,473.00	$31,343.00	$61,816.00
Shop support	$43,973.00	$4,070.00	$48,043.00
IDC (.26) - not equipment	$54,503.41	$83,727.28	$138,230.69
	$264,131.91	$405,755.28	$669,887.19
			$669,887.19
Note: salaries are average salary			

Budget Justification

Salaries are for 3 beamline scientists. One will be in Chicago at the APS for the full year. Two will be assigned to the NSLS II for the first half of the year, during the construction and installation phase, and continue during operations.

An electronics support person (part time), William Heubsch, for $25,000. He was the person that built the electronic platform that is currently used. He is extremely valuable in setting up the new facilities and will continue to be valuable as the system transforms

to an operation mode.

Fringe benefits is at 45% of salaries.

No equipment funds are requested

Material and supplies, Total: $61,816
With the following distribution and purpose:

Item	Count/Justification	APS	NSLS II
Cold Light Lamp Source	Replacement for broken lamps of binocular microscope (KL 1600)		$1,077.00
Kim Wipes	36 pk normal and XL	$573.00	$341.00
Tweezers	Set of 10	$35.00	$30.00
Cotton-Tipped Applicators	20 Pk	$300.00	$210.00
Methanol/Ethanol/Acetone/Isopropanol	4L bottles	$300.00	$300.00
Turpenoid	4L bottles		$55.00
Polyethylene Sample Vials	200 ct	$200	
Needles+Holders	36 ct	$60.00	$100.00
Mounting epoxy Stycast	Single use portions 60 uses		$648.00
Agate Mortar and Pestle sets	2	$180.00	$180.00
Diamonds (DAC)	6 anvils ($850/anvil)		$5,100.00
Gasket material	Rhenium (100 mmx100mm), Tungsten (100 mmx100 mm)		$2,052.00
Sintered diamond anvils (MAC)	30/20	$10,125.00	$6,750.00
WC anvils/backing plates	60/50	$12,000.00	$10,000.00
DIA cells	35 for DIA/60 for DDIA/25 for DT25	$4,700.00	$2,000.00
Type D thermocouple		$2,000.00	$500.00
LSNH cables and connectors	NSLS II safety standards require all new cables that		$2,000.00

	are low-smoke-zero-halogens. This is expensive cabling		
		$30,473.00	$31,343.00
			$61,816.00

Other costs, Shop charges total: $48,403

Shop charges: We budget for 4 hours per week of mechanical and electrical shop support for the APS program at $180/hour (total $37,440) and $6,533 for rigger charges to move heavy objects related to the experiments. This is required for set up and maintenance of the facility that is distant from our home base at Stony Brook. We include $4070 for shop charges at the NSLS II. This will allow 22.6 hours of support for system installation.

Travel $20,800

Travel is budgeted as follows:

	APS	NSLS II
COMPRES Annual Meeting 3 scientist + 3 PIs covering transportation to the meeting 800/person	$1,600.00	$3,200.00
Travel and registration for one conference for each of the three beamline scientist 2000/pp	$2,000.00	$4,000.00
Travel SBU-CHI support staff and beamline scientist 10 trips 1000/trip	$10,000.00	
	$13,600.00	$7,200.00
		$20,800.00

Indirect costs: 26% of modified direct costs (off campus rate).

Appendices

Publication List

2014

Bollinger, C., Raterron, P., Cordier, P., Merkel, S. (2014), Polycrystalline olivine rheology in dislocation creep: revisiting experimental data to 8.1 GPa, , Phys. Earth Planet. Int. , 228, 211-219., doi: http://dx.doi.org/10.1016/j.pepi.2013.12.001.

Cayman, T. U., E. K. Jason, S. P. Jeffrey, M. R. Daniel, and R. P. Wendy (2014), The Role of Carbon in Extrasolar Planetary Geodynamics and Habitability, The Astrophysical Journal, 793(2), 124.

Chen, H., J. Burnett, F. Zhang, J. Zhang, H. Paholak, and D. Sun (2014a), Highly crystallized iron oxide nanoparticles as effective and biodegradable mediators for photothermal cancer therapy, Journal of Materials Chemistry B, 2(7), 757-765, doi:10.1039/C3TB21338B.

Chen, J. C., T Yu, S Huang, J Girard, X Liu (2014), Compressibility of Liquid FeS Measured Using X-ray Radiograph Imaging, , Phys. Earth Planet. Interiors, 228, 294-299

Chen, S., et al. (2014b), Structural transformation of confined iodine in the elliptical channels of AlPO4-11 crystals under high pressure, Physical Chemistry Chemical Physics, 16(18), 8301-8309, doi:10.1039/C3CP55164D.

Cong, R., X. Liu, H. Cui, J. Zhang, X. Wu, Q. Wang, H. Zhu, and Q. Cui (2014), The plasma assisted synthesis and high pressure studies of the structural and elastic properties of metal nitrides XN (X = Sc, Y), CrystEngComm, 16(19), 3977-3985, doi:10.1039/C3CE42643B.

Dai, L., Karato, S. (2014a), The effect of pressure on hydrogen-assisted electrical conductivity of olivine: implications for the conductivity jump at 410-km, Phys. Earth Planet. Inter. in press, 232: 51-56.

Dai, L., Karato, S. (2014b), High and highly anisotropic electrical conductivity of the asthenosphere caused by hydrogen diffusion in olivine Earth and Planetary Science Letters, in press.

Dai, L., Karato, S. (2014c), The effect of oxygen fugacity on hydrogen-assisted electrical conductivity of olivine: implications for the mechanism of conduction, Phys. Earth Planet. Inter. , 232: 57-60.

Dai, L., Karato, S. (2014d), The effects of Fe and H on the electrical conductivity of olivine, Phys. Earth Planet. Inter., in press.

Dixon, N. A. (2014), Experimental Constraints on the Rheological Behavior of Olivine at Upper Mantle Conditions, Ph. D. thesis, 125 pp, Massachusetts Institute of Technology.

Dong, H., S. Dorfman, J. Wang, D. He, and T. Duffy (2014), The strength of ruby from X-ray diffraction under non-hydrostatic compression to 68 GPa, Physics and Chemistry of Minerals, 41(7), 527-535, doi:10.1007/s00269-014-0664-2.

Du, W., L. Li, and D. J. Weidner (2014), Experimental observation on grain boundaries affected by partial melting and garnet forming phase transition in KLB1 peridotite, Physics of the Earth and Planetary Interior(228), 287-293.

Fan, D., S. Wei, M. Ma, Z. Chen, B. Li, and H. Xie (2014), High-pressure elastic behavior of Ca4La6(SiO4)6(OH)2 a synthetic rare-earth silicate apatite: a powder X-ray diffraction study up to 9.33 GPa, Physics and Chemistry of Minerals, 41(2), 85-90, doi:10.1007/s00269-013-0626-0.

Farla, R., Amulele, G., Girard, J., Miyajima, N. and Karato, S., (2014), High pressure and temperature deformation experiments on polycrystalline wadsleyite using the rotational Drickamer apparatus, submitted to Physics and Chemistry of Minerals.

Girard, J., G. Amulele, R. Farla, A. Mohiuddin, and S. Karato (2014), In-situ deformation experiments of bridgmanite + (Mg,Fe)O under the lower mantle conditions, Nature, submitted.

Girard, J. a. K., S. (2014), Evidence and implications of the limited depth range of a metallic-Fe-bearing layer in the lower mantle, submitted to Nature.

Gong, C., et al. (2014), Structural Phase Transition and Photoluminescence Properties of YF3:Eu3+ Nanocrystals under High Pressure, The Journal of Physical Chemistry C, 118(39), 22739-22745, doi:10.1021/jp504474u.

Hong, X., L. Ehm, and T. S. Duffy (2014a), Polyhedral units and network connectivity in GeO2 glass at high pressure: An X-ray total scattering investigation, Applied Physics Letters, 105(8), 081904, doi:doi:http://dx.doi.org/10.1063/1.4894103.

Hong, X., M. Newville, T. S. Duffy, S. R. Sutton, and M. L. Rivers (2014b), X-ray absorption spectroscopy of GeO2 glass to 64 GPa, Journal of Physics-Condensed Matter, 26(3), doi:035104 10.1088/0953-8984/26/3/035104.

Huang, F., Q. Zhou, L. Li, X. Huang, D. Xu, F. Li, and T. Cui (2014a), Structural Transition of MnNb2O6 under Quasi-Hydrostatic Pressure, The Journal of Physical Chemistry C, 118(33), 19280-19286, doi:10.1021/jp503542y.

Huang, S., and J. Chen (2014), Equation of state of pyrope–almandine solid solution measured using a diamond anvil cell and in situ synchrotron X-ray diffraction, Physics of the Earth and Planetary Interiors, 228, 88-91, doi:http://dx.doi.org/10.1016/j.pepi.2014.01.014.

Huang, X., D. Duan, F. Li, Y. Huang, L. Wang, Y. Liu, K. Bao, Q. Zhou, B. Liu, and T. Cui (2014b), Structural stability and compressive behavior of ZrH2 under hydrostatic pressure and nonhydrostatic pressure, RSC Advances, 4(87), 46780-46786, doi:10.1039/C4RA06713D.

Huang, Y., X. Huang, Z. Zhao, W. Li, S. Jiang, D. Duan, K. Bao, Q. Zhou, B. Liu, and T. Cui (2014c), Experimental verification of the high pressure crystal structures in NH3BH3, The Journal of Chemical Physics, 140(24), 244507, doi:doi:http://dx.doi.org/10.1063/1.4884819.

Hunt, S., A. M. Walker, O. Lord, S. Stackhouse, L. Armstrong, A. Parsons, G. Lloyd and M. Whitaker (2014a), Anelasticity of the HCP metal Zinc: a key to understanding the dynamics of Earth's core, abstract DI31A-4252, in AGU fall meeting, edited.

Hunt, S. A., A. M. Walker and E. Mariani (2014b), Rate of texture development in post-perovskite in PPV@10 a meeting to celebrate the tenth anniversary of the discovery of post-perovskite. , edited, Bristol, UK.

Hunt, S. A., Weidner, D. J., McCormack, R. J., Whitaker, M. L., Bailey, E., Li, L., Vaughan, M. T., Dobson, D. P. (2014c), Deformation T-Cup: A new multi-anvil apparatus for controlled strain-rate deformation experiments at pressures above 18 GPa. , Rev. Sci. Instrum. , 85, 085103, doi:10:1063/1.4891338.

Karato, S. (2014a), Asymmetric shock heating and the terrestrial magma ocean origin of the Moon, , Proceedings of the Japan Academy, B90: 97-103.

Karato, S. (2014b), Does partial melting explain geophysical anomalies?, Physics of the Earth and Planetary Interiors, 228, 300-306.

Karato, S. (2014c), Some remarks on the models of plate tectonics on terrestrial planets: From the view-point of mineral physics, Tectonophysics, 631, 4-13.

Karato, S., Olugboji, T., and Park, J. (2014d), Origin of the mid-lithosphere discontinuity, submitted to Nature Geoscience.

Kung, J., B Li. (2014), Lattice Dynamic Behavior of Orthoferrosilite (FeSiO3) toward Phase Transition under Compression, , J. Phys. Chem. C 118(23), , 12410-12419

Lang, M., F. Zhang, J. Zhang, C. L. Tracy, A. B. Cusick, J. VonEhr, Z. Chen, C. Trautmann, and R. C. Ewing (2014), Swift heavy ion-induced phase transformation in Gd2O3, Nuclear Instruments and Methods in Physics Research Section B: Beam Interactions with Materials and Atoms, 326, 121-125, doi:http://dx.doi.org/10.1016/j.nimb.2013.10.073.

Li, B., R Liebermann (2014), Study of the Earth's Interior Using Measurements of Sound Velocities in Minerals by Ultrasonic Interferometry, Phys. Earth Planet. Interiors, 233, 135-153

Li, D., X. Wu, J. Jiang, X. Wang, J. Zhang, Q. Cui, and H. Zhu (2014a), Pressure-induced phase transitions in rubidium azide: Studied by in-situ x-ray diffraction, Applied Physics Letters, 105(7), 071903, doi:doi:http://dx.doi.org/10.1063/1.4893464.

Li, G., Y. Li, M. Zhang, Y. Ma, Y. Ma, Y. Han, and C. Gao (2014b), Pressure-induced isostructural phase transition in CaB4, RSC Advances, 4(80), 42523-42529, doi:10.1039/C4RA04102J.

Li, L., and D. Weidner (2014), Detection of melting by X-ray imaging at high pressure, Review of Scientific Instruments, doi:10.1063/1.4880730(85), 4.

Li, Q., B. Cheng, B. Tian, R. Liu, B. Liu, F. Wang, Z. Chen, B. Zou, T. Cui, and B. Liu (2014c), Pressure-induced phase transitions of TiO2 nanosheets with high reactive {001} facets, RSC Advances, 4(25), 12873-12877, doi:10.1039/C3RA46404K.

Li, Q., H. Zhang, B. Cheng, R. Liu, B. Liu, J. Liu, Z. Chen, B. Zou, T. Cui, and B. Liu (2014d), Pressure-induced amorphization in orthorhombic Ta2O5: An intrinsic character of crystal, Journal of Applied Physics, 115(19), 193512, doi:doi:http://dx.doi.org/10.1063/1.4879245.

Lord, O. T., E. Wan, S. A. Hunt, A. M. Walker, J. Santangeli, M. J. Walter, D. P. Dobson, I. G. Wood, L. Vočadlo, G. Morard and M. Mezouar (2014), The NiSi melting curve to 70 GPa, Physics of the Earth and Planetary Interiors, 233, 13-23, doi:doi:10.1016/j.pepi.2014.05.005.

Machon, D., P. F. McMillan, A. San-Miguel, P. Barnes, and P. T. Hutchins (2014), Semiconductor Clathrates: In Situ Studies of Their High Pressure, Variable Temperature and Synthesis Behavior, in The Physics and Chemistry of Inorganic Clathrates, edited by G. S. Nolas, pp. 91-123, Springer Netherlands, doi:10.1007/978-94-017-9127-4_4.

Meng, X.-X., et al. (2014), Structural stability and electrical properties of AlB 2 -type MnB 2 under high pressure, Chinese Physics B, 23(1), 016102.

Miyagi, L., G. Amulele, K. Otsuka, Z. Du, R. Farla, and S. Karato (2014), Plastic anisotropy and slip systems in ringwoodite deformed to high strainin the rotational Drickamer apparatus, Physics of the Earth and Planetary Interiors, 228, 244-253.

Olugboji, T., Park, J., Karato, S., Kawakatsu, H. and Shinohara, M. (2014), The nature of the lithosphere-asthenosphere boundary in the normal oceanic upper mantle submitted to Geochemistry, Geophysics and Geosystems.

Otsuka, K., and Karato, S. (2014), The influence of ferric iron and hydrogen on the Fe-Mg inter-diffusion in (Mg,Fe)O ferropericlase in the lower mantle, Physics and Chemistry of Minerals, in press.

Raterron, P., Detrez, F.,Castelnau, O., Bollinger C., Merkel, S., Cordier, P. (2014), Multiscale Modeling of Upper Mantle Plasticity: from Single-Crystal Rheology to Multiphase Aggregate Deformation, , Phys. Earth Planet. Int. , 228, 232-243. , doi:10.1016/j.pepi.2013.11.012.

Selway, K. M., Yi, J. and Karato, S. (2014), Water content of the Tanzanian lithosphere: Implications for cratonic growth and stability, Earth Planet. Sci. Lett. , 388: 175-186.

Sun, Y., J. Chen, V. Drozd, A. Durigin, S. Najiba, and X. Liu (2014), Phase boundary of pressure-induced I4mm to Cmc21 transition in ammonia borane at elevated temperature determined using Raman spectroscopy, International Journal of Hydrogen Energy, 39(16), 8293-8302, doi:http://dx.doi.org/10.1016/j.ijhydene.2014.03.070.

Tang, R., Y. Li, N. Li, D. Han, H. Li, Y. Zhao, C. Gao, P. Zhu, and X. Wang (2014), Reversible Structural Phase Transition in ZnV2O6 at High Pressures, The Journal of Physical Chemistry C, 118(20), 10560-10566, doi:10.1021/jp411283m.

Unterborn, C. T., J. E. Kabbes, J. S. Pigott, D. M. Reaman, and W. R. Panero (2014), THE ROLE OF CARBON IN EXTRASOLAR PLANETARY GEODYNAMICS AND HABITABILITY, Astrophysical Journal, 793(2), doi:124 10.1088/0004-637x/793/2/124.

Wang, S. M., J. Z. Zhang, D. W. He, Y. Zhang, L. P. Wang, H. W. Xu, X. D. Wen, H. Ge, and Y. S. Zhao (2014), Sulfur-catalyzed phase transition in MoS2 under high pressure and temperature, Journal of Physics and Chemistry of Solids, 75(1), 100-104, doi:10.1016/j.jpcs.2013.09.001.

Wang, S. Y., XH; Zhang, JZ; Zhang, Y; Wang, LP; Leinenweber, K; Xu, HW; Popov, D; Park, C; Yang, WG; He, DW; Zhao, YS (2014), Crystal structures, elastic properties, and hardness of high-pressure synthesized CrB2 and CrB4., JOURNAL OF SUPERHARD MATERIALS 36, 279-287 doi:10.3103/S1063457614040066.

Weidner, D., J., and L. Li (2014), Kinetics of Melting in Peridotite from Volume Strain Measurements, Physics of the Earth and Planetary Interior, submitted.

Wu T, Tyson T A, Chen H, Gao P, Yu T, Chen Z, Liu Z, Ahn K H, W. X, and C. S-W (2014), Pressure dependent structural changes and predicted electrical polarization in perovskite RMnO3, arXiv:1403.7998 [cond-mat]

Xi, X., et al. (2014), Bulk Signatures of Pressure-Induced Band Inversion and Topological Phase Transitions in ${\mathrm{Pb}}_{1\ensuremath{-}x}{\mathrm{Sn}}_{x}\mathrm{Se}$, Physical Review Letters, 113(9), 096401.

Xu, H., C. Li, D. He, and Y. Jinag (2014), Stability and structure changes of Na-titanate nanotubes at high temperature and high pressure, Powder Diffraction, 29(02), 147-150, doi:doi:10.1017/S0885715614000220.

Yang, X., et al. (2014a), A novel pressure-induced phase transition in CaZrO3, CrystEngComm, 16(21), 4441-4446, doi:10.1039/C3CE42590H.

Yang, X., Q. Li, R. Liu, B. Liu, H. Zhang, S. Jiang, J. Liu, B. Zou, T. Cui, and B. Liu (2014b), Structural phase transition of BaZrO3 under high pressure, Journal of Applied Physics, 115(12), 124907, doi:doi:http://dx.doi.org/10.1063/1.4868906.

Yin, G., H. Yin, X. Wang, M. Sun, L. Zhong, R. Cong, H. Zhu, W. Gao, and Q. Cui (2014), Mg doping effect on high-pressure behaviors of apatite-type lanthanum silicate, Journal of Alloys and Compounds, 611, 24-29, doi:http://dx.doi.org/10.1016/j.jallcom.2014.05.122.

Yu T, Tyson T A, Chen H Y, Abeykoon A M M, C. Y-S, and A. K. H (2014), Nature of structural changes near the magnetic ordering temperature in small-ion rare earth perovskites RMnO3, arXiv:1403.4807 [cond-mat]

Yu, T., T. A. Tyson, H. Y. Chen, A. M. M. Abeykoon, Y. S. Chen, and K. H. Ahn (2014a), Absence of significant structural changes near the magnetic ordering temperature in small-ion rare earth perovskite R MnO 3, Journal of Physics: Condensed Matter, 26(49), 495402.

Yu, T., T. A. Tyson, P. Gao, T. Wu, X. Hong, S. Ghose, and Y. S. Chen (2014b), Structural changes related to the magnetic transitions in hexagonal $\mathrm{InMn}{\mathrm{O}}_{3}$, Physical Review B, 90(17), 174106.

Zhang, J., H. Cui, P. Zhu, C. Ma, X. Wu, H. Zhu, Y. Ma, and Q. Cui (2014), Photoluminescence studies of Y2O3:Eu3+ under high pressure, Journal of Applied Physics, 115(2), 023502, doi:doi:http://dx.doi.org/10.1063/1.4861386.

Zhang, J., J Han, J Zhu, Z Lin, M Braga, L Daemen, L Wang, Y Zhao (2014), High Pressure-High Temperature Synthesis of Lithium-rich Li3O(Cl, Br) and Li3 − xCax/2OCl Anti-Perovskite Halides Inorg. Chem. Comm.,, 48, 140-143 doi:10.1016/j.inoche.2014.08.036.

Zhao, J., and L. Yang (2014), Structure Evolutions and Metallic Transitions in In2Se3 Under High Pressure, The Journal of Physical Chemistry C, 118(10), 5445-5452, doi:10.1021/jp4076383.

Zheng, W., Z. C. Feng, J.-F. Lee, D.-S. Wuu, and R. S. Zheng (2014), Lattice deformation of wurtzite MgxZn1−xO alloys: An extended X-ray absorption fine structure study, Journal of Alloys and Compounds, 582, 157-160, doi:http://dx.doi.org/10.1016/j.jallcom.2013.08.021.

Zou, Y., X Qi, X Wang, T Chen, X Li, D Welch, B Li (2014), High-pressure Behavior and Thermoelastic Properties of Niobium Studied by in situ X-ray Diffraction, , J. Appl. Phys. , 116, 013516.

2015

Bollinger, C., S Merkel, P Cordier, P Raterron (2015), Deformation of Forsterite Polycrystals at Mantle Pressure: Comparison with Fe-bearing Olivine and the Effect of Iron on its Plasticity, *Phys. Earth Planet. Interiors, in press*, *240, 95-104*.

Dorfman, S. M., S. R. Shieh, and T. S. Duffy (2015), Strength and texture of Pt compressed to 63 GPa, *Journal of Applied Physics*, *117*(6), 065901, doi:doi:http://dx.doi.org/10.1063/1.4907866.

Drozd, V., A. Durygin, S. Saxena, V. E. Antonov, and M. Tkacz (2015), Properties of Ti3AlH6 and Ti3AlD6 systems at high pressure studied by synchrotron X-ray diffraction analysis, *Journal of Alloys and Compounds*, *619*, 78-81, doi:http://dx.doi.org/10.1016/j.jallcom.2014.09.039.

Girard, J., G. Amulele, R. Farla, and S. Karato (2015), Shear deformation experiment of bridgmanite + magnesiowüstite aggregates under the lower mantle conditions, *Science in press*.

Huang, S. (2015), Influence of Chemical Composition and Water on the Bulk Modulus of Pyrope,, Florida International University, Miami.

Jaret, S. J., W. R. Woerner, B. L. Phillips, L. Ehm, H. Nekvasil, S. P. Wright, and T. D. Glotch (2015), Maskelynite formation via solid-state transformation: Evidence of infrared and X-ray anisotropy, *Journal of Geophysical Research: Planets*, *120*(3), 570-587, doi:10.1002/2014JE004764.

Karato, S. (2015), Water in the evolution of Earth and other terrestrial planets, Treatise on Geophysics, in *Evolution of the Earth*, edited by e. b. D. J. Stevenson, pp. 105-144, Elsevier, in press.

Khan, T. (2015), High Pressure and High Temperature Study of Magnesiochromite and Its Geophysical Implications, The University of Western Ontario, London.

Li, H., Y. Li, N. Li, Y. Zhao, H. Zhu, P. Zhu, and X. Wang (2015a), A comparative study of high pressure behaviors of pyrochlore-type and thortveitite-type In2Ge2O7, *RSC Advances*, *5*(55), 44121-44127, doi:10.1039/C5RA04587H.

Li, Y., Y. Zou, T. Chen, X. Wang, X. Qi, H. Chen, J. Du, and B. Li (2015b), P-V-T equation of state and high-pressure behavior of CaCO3 aragonite, American Mineralogist, Volume 100, pages 2323–2329, 2015. , *American Mineralogist*, *100*, 2323–2329.

Panero, W. R., J. S. Pigott, D. M. Reaman, J. E. Kabbes, and Z. Liu (2015), Dry (Mg,Fe)SiO3 perovskite in the Earth's lower mantle, *Journal of Geophysical Research: Solid Earth*, *120*(2), 894-908, doi:10.1002/2014JB011397.

Serra-Crespo, P., A. Dikhtiarenko, E. Stavitski, J. Juan-Alcaniz, F. Kapteijn, F.-X. Coudert, and J. Gascon (2015), Experimental evidence of negative linear compressibility in the MIL-53 metal-organic framework family, *CrystEngComm*, *17*(2), 276-280, doi:10.1039/C4CE00436A.

Wang, S. M., et al. (2015a), A New Molybdenum Nitride Catalyst with Rhombohedral MoS2 Structure for Hydrogenation Applications, *Journal of the American Chemical Society*, *137*(14), 4815-4822, doi:10.1021/jacs.5b01446.

Wang, S. M., et al. (2015b), Revisit of Pressure-Induced Phase Transition in PbSe: Crystal Structure, and Thermoelastic and Electrical Properties, *Inorganic Chemistry*, *54*(10), 4981-4989, doi:10.1021/acs.inorgchem.5b00591.

Xiao, G., X. Yang, K. Wang, X. Huang, Z. Ding, Y. Ma, G. Zou, and B. Zou (2015), A Protocol to Fabricate Nanostructured New Phase: B31-Type MnS Synthesized under High Pressure, *Journal of the American Chemical Society*, *137*, 102971-110303.

Xiong, Z., X. Liu, S. Shieh, F. Wang, X. Wu, X. Hong, and Y. Shi (2015), Equation of state of a synthetic ulvöspinel, (Fe1.94Ti0.03)Ti1.00O4.00, at ambient temperature, *Physics and Chemistry of Minerals*, *42*(3), 171-177, doi:10.1007/s00269-014-0704-y.

Zhang, F. X., M. Lang, and R. C. Ewing (2015a), Atomic disorder in Gd2Zr2O7 pyrochlore, *Applied Physics Letters*, *106*(19), 191902, doi:doi:http://dx.doi.org/10.1063/1.4921268.

Zhang, H., T. Yu, Z. Chen, C. Nelson, L. Bezmaternykh, A. Abeykoon, and T. Tyson (2015b), Probing Magnetostructural Correlations in Multiferroic HoAl3(BO3)4, *Physical Review B*, *92*, 104108.

Zhang, J., J. Zhu, L. Wang, and Y. Zhao (2015c), A new lithium-rich anti-spinel in Li-O-Br system, *Chemical Communications*, *51*(47), 9666-9669, doi:10.1039/c5cc01109d.

Zhao, R., P. Wang, B.-b. Yao, T.-t. Hu, T.-y. Yang, B.-x. Xiao, S.-m. Wang, C.-h. Xiao, and M.-z. Zhang (2015), Co effect on zinc blende-rocksalt phase transition in CdS nanocrystals, *RSC Advances*, *5*(23), 17582-17587, doi:10.1039/C4RA14798G.

Zhou, B., G. Xiao, X. Yang, Q. Li, K. Wang, and Y. Wang (2015), Pressure-dependent optical behaviors of colloidal CdSe nanoplatelets, *Nanoscale*, *7*(19), 8835-8842, doi:10.1039/C4NR07589G.

Zou, Y., X. Wang, T. Chen, X. Li, X. Qi, D. Welch, P. Zhu, B. Liu, T. Cui, and B. Li (2015), Hexagonal-structured ε-NbN: ultra-incompressibility, high shear rigidity, and a possible hard superconducting material, *Sci. Rep.*, *5*, doi:10.1038/srep10811.

Vision for NSLS II

High Pressure Studies of Earth Materials at the National Synchrotron Light Source II

A vision for High Pressure Studies at Brookhaven National Lab

The High Pressure Village

Major experimental facilities at Brookhaven National Laboratory (BNL) - the National Synchrotron Light Source II (NSLS II) and the Center for Functional Nanomaterials (CFN) - will be at the forefront of condensed matter science over the next decade, and provide the foundation upon which to build world leading research and development programs for the investigation of materials at extreme pressure and temperature conditions. The NSLS-II became

operational in October, 2014 and has begun scientific experiments on a sparse schedule on six beamlines. Other beamlines are under construction, slated to open over the next three years, with even more slated to come alive over the next decade.

Here we outline the vision for a flexible platform, the High Pressure Village, for high pressure Earth science research that is well matched to current and future capabilities at the NSLS II. This vision goes beyond the single project beamline on which we have so far been awarded real estate and beam time for diffraction experiments with both large volume and diamond anvil cell high pressure systems and the scheduled IR beamline where we have considerable access. We are making proposals for using some of the next beamlines that are funded, but not yet completely designed. We also want to indicate related, Brookhaven based, facilities that may be useful to high pressure scientists for other in situ experiments or for sample analysis after the experiment. NSLS II, along with affiliated facilities, bring a unique set of tools. We feel that this is an opportunity to continue existing research programs and to conceive and execute new ones. We stand open for suggestions, advice, and help to amend the vision and to bring it to reality.

The High Pressure Village provides world-class experimental tools and technical support to the scientific community through a peer reviewed proposal system. These facilities are based on established partnerships between participating research Institutions (including Stony Brook University and Carnegie Institution of Science), COMPRES, and Brookhaven National Laboratory. We envision a program that allows a comprehensive investigation of materials at extreme conditions employing frontier sample preparation techniques as well as *in situ* and *ex situ* experimental capabilities. The program spans two user facilities, NSLS II and CFN, augmented by the capabilities available at the Mineral Physics Institute (MPI) at Stony Brook University (SBU). At the core of the program are x-ray beamlines that enable diffraction and imaging on samples at pressures from the subsurface to the center of the Earth and a diamond anvil cell enabled IR beamline that facilitates studies at extremes of pressure and temperature. Under the broader umbrella, there are world-class tools to define major and minor element distribution with extremely high spatial resolution, inelastic beamlines capable of world leading energy resolution, XANES and EXAFS capabilities that define atom coordination for the major Earth elements, Si, Mg, and Al for very small samples, and high pressure synthesis tools.

The philosophy of the High Pressure Village is to provide user access to a broad range of high pressure tools that span the standard range of high pressure experimentation and then to add focus to a few issues that create a unique scientific environment for high pressure studies. The direction of this added focus will be defined by the PI's in collaboration with an advisory council and the user community, considering the unique opportunities offered by the new NSLS II synchrotron.

The High Pressure Village will enable world - leading contributions to the following Earth science issues:
Stress – strain – time for Earth materials

- Rheological properties at P, T
- Elastic, anelastic, plastic properties from MHz to mHz
- Kinetics of phase transformations and effects on Q

Atomic structure

- Crystalline phases
- Liquids and amorphous materials
- Cation coordination, order – disorder

Extreme petrology

- Petrology of the Earth
- Solidus of the lower mantle
- Water in the Earth
- Other volatiles in the Earth

Properties of melts

- Thz to mhz elastic, viscous properties

- Equation of state

Rock mechanics

- Carbon sequestration
- Mechanical and chemical interaction of rocks and fluids
- Earthquake faulting
- Physics of fracking

Realizing the Vision

The program outlined above is guided by the outcomes of the three strategic planning workshops for Materials at Extreme Conditions since 2008, held as part of the development of the NSLS-II's beamline portfolio and strategic plan. With the completion of the NSLS II construction and the building of the first six beamlines, this vision is coming into existence. Here we define the materialization of the hopes as distributed over the next few years.

In Progress:

The base experimental capabilities for a successful program on Materials at Extreme Conditions are being built now. The high pressure community has been successful in establishing a foothold at NSLS-II. We have finalized a Partner User relationship on beamline XPD, the high energy powder diffraction beamline, one of the first six beamlines open for business. This agreement provides experimental space in a very large hutch to house the diamond cell program and a 1000 ton press driving the multi-anvil program.

The proposal for "Frontier Synchrotron Infrared Spectroscopy" (**FIS**) beamline has been approved as one of eight beamlines to be developed and constructed at NSLS-II over the next two years. One of the prominent FIS capabilities is synchrotron infrared spectroscopy at high pressure and temperature. Until the synchrotron beamline is in place, infrared experiments can be done in the hutch using a lab style glow bar light source. A general user review system is used to allocate beamtime with some set-aside time specifically allocated to COMPRES users.

Installation and Construction

<u>High Pressure Diffraction Program at XPD-D</u>

The first capabilities to investigate materials at extreme pressure and temperature conditions will be established at the X-ray Powder Diffraction (XPD) beamline. The XPD beamline, located at one of the three damping wigglers at NSLS-II, provides ideal beam characteristics in the energy range from 30-70 keV for diffraction studies of materials enclosed in complex sample environments. The optical layout of the XPD beamline allows two operational modes, a high-flux ($\Delta E/E \sim 1.1\times10^{-3}$) or a high resolution ($\Delta E/E \sim 2\times10^{-4}$) configuration. The beam size at the sample position in hutch C can be varied 2□0.7 (h) × 1□0.05 (v) mm^2 (FWHM) by vertically focusing with a mirror and horizontally with the sagittal-bend double Laue monochromator. The fully focused beam at the sample position in hutch C of XPD creates a virtual source that will be re-focus in hutch D using a K-B mirror system. We expect a minimum beam size at the DAC sample position in XPD-D of 5 × 5 μm^2 with a photon flux of about 6.25×10^{10} ph/s at 50 keV. The focal spot is sufficiently small to allow for efficient laser heating in a DAC experiment, but large enough to allow quantitative analysis of the powder diffraction patterns.

The diamond anvil cell system will initially be based on the transferred equipment of the NSLS beamlines X17B3 and X17C. This includes, Huber sample and detector positioning stages, a K-B mirror system, a Perkin-Elmer XRD1620 area detector, a compact double-sided laser heating system with temperature measurement, pressure controller for membrane driven diamond anvil cells, an offline Raman system, and a functional support laboratory for sample loading.

The experimental system provides a flexible base for angle dispersive diffraction experiments in diamond anvil cells at ambient and high temperatures and is a solid base for further technical development of the DAC program. The

diamond anvil system will include in situ laser heating with the x-ray spot as small as 5 x 5 μm^2. We will make a number of changes to the setup during initial installation of the system at XPD-D: (i) the offline Raman system will be repurposed and rebuild as an online ruby system, to take full advantage of the membrane driven diamond anvil cell capabilities and increase user throughput, (ii) increase the stability of the laser heating system and fully integrate the temperature measurements, and (iii) increase the user friendliness of the beamline control system in collaboration with the NSLS-II controls group.

The partnership with XPD will provide the high pressure program with access to the large number of detectors at XPD-1 including additional area detectors, CdTe-based pixel array detectors and point detectors. This will allow us to provide more detector options for users that cannot be covered by the proposed standard setup.

We have a pending NSF-MRI proposal to fully upgrade the diamond anvil cell system from the base to the diamond anvil cell; including an optimized K-B mirror system, new detectors, and a new sample position system.

The experimental setup will serve the majority of the previous user community of the NSLS-DAC program and is able provide experimental capabilities for users who want to conduct a wide range of high PT diffraction experiments. We will offer state-of-the art angle dispersive X-ray diffraction capabilities in the energy range of 30-70 keV, which will allow our users to study P, T equations-of-state, phase transitions, compression behavior, stability field, etc.

The experiments in the multi-anvil cell system (MAC), especially the imaging of the sample, will benefit from the parallel beam geometry at XPD that can be achieved through the combination of the double-Laue monochromator and a 1.3 m focusing mirror. The monochromatic beam will provide a variety of new experimental capabilities for the MAC user community, e.g. quantitative analysis of diffraction intensities, analysis of "spotty" diffraction patterns using multi-grain approaches - to provide 3D-XRD for grain maps and grain dynamics at high PT - and potentially combined tomographic imaging and diffraction experiments.

The multi-anvil system will consist of a 1000 ton press driving a DT-25 guideblock, a DDIA guideblock, or a T-10 guideblock. The DT-25 is a new system, never before used at a synchrotron, that is a Kawai styled guideblock, using 25 mm cubic anvils, that has been modified by adding a uniaxial stress capability. The DDIA (on loan from UNLV through Pamela Burnley) is the same style of guideblock that was used at the old NSLS. The T-10 is also inherited from the NSLS, being a Kawai styled system with 10 mm cubes. These systems will use monochromatic x-rays and be capable of defining stress, and strain as a function of time. We estimate stress can be defined to levels of about 10 MPa and strain can be measured to about 10^{-5}. One specialty of the NSLS II system will be the focus on stress – strain – time characterizations. We will focus on system control software and data analysis software to optimize resolution of these variables enabling rheology, elasticity, anelasticity, kinetics, and other similar measurements.

The high energy (50-70 kev) beam at XPD opens new opportunities for a unique and competitive scientific program. The high pressure capabilities at XPD-D will allow the users to conduct a wide range of experiments in a DAC or MAC. The spatial resolution of the diffraction data that can be collected at both experiments in XPD-D is sufficient for precise determination of the p-V-T equation-of-state of Earth materials. The combination of laser-heating or resistive heating in a DAC and MAC will enable the users to investigate their samples over a large pressure and temperature space. This covers experiments to study phase transition, reactions between minerals, melting in minerals, exploration of stability fields, partitioning in partially molten system and many more.

While we intend to build a program that serves a very broad user community, we will develop the DAC instrument to be best in class in investigation of atomic structure at high pressure and temperature. The high energy X-ray beam that the dampening wiggler at XPD provides, gives the program a distinct advantage for the investigation of the atomic structure of crystalline, disordered, nanocrystalline, amorphous or liquid Earth material compared to other

established high pressure beamlines. The DAC limits by design the access to the reciprocal space; high energy X-rays allow us to partially overcome this restriction and measure a larger amount of the reciprocal space, which results in more precise and reliable parameters in the structure solution and refinement independent of the state of the sample being powder, single-crystal or liquid.

A second focus theme that serves both the DAC and MAC community is the Diffraction Microscopy (3DXRD) technique or so-called 'multigrain technique.' The sample is illuminated by a full field beam and 2D transmission diffraction images are taken as the sample is rotated. Using a large area farfield detector (e.g Perkin-Elmer area detector) and reconstruction software, the full orientation, elastic strain tensor, center of mass (5-10 microns), and unit cell refinement can be determined for every grain within the illuminated volume (for sufficiently coarse grains). While a full 3D reconstruction of the grain structure will not be possible with this initial setup, valuable data on elastic strain distribution (therefore stress) over different grains as well as grain rotation paths and potentially structure refinements of individual grains at pressure, temperature and stress can be obtained. Once the feasibility of 3DXRD measurement has been proven, we will pursue the funding of a semi-transparent near field detector to upgrade the experimental setup. NSLS-II is developing the 3DXRD technique for use at XPD-1, HRX and HEX, which will significantly benefit our proposed development of 3DXRD for high pressure and temperature experiments. We are fully aware of similar developments at currently going on at other synchrotron sources such as ALS, APS, CHESS and ESRF and intend to reach out to these programs. We feel that the development of the 3DXRD technique at high pressure is a high-risk high-return effort that has a potential for transformative science. It will enable the investigation of complex systems, closer to real rocks and aggregates. The ability to collect grain-by-grain kinetics on a statistically significant number of grains rather than just measuring a powder-averaged value, will allow more realistic models to be developed that incorporate the true kinetic distributions of behavior due to the inhomogeneous nature of all polycrystalline materials.
Thirdly, we will endeavor to develop imaging techniques such as phase contrast imaging, or diffraction enhanced imaging that promise to produce high-contrast 2D or 3D (by rotating the sample) images. This will enable studies that are concerned with grain boundary morphology or movement at pressure, temperature and stress. While these techniques are being developed and used at other synchrotrons, the coherence of the NSLS II source promises to provide higher spatial resolution. Furthermore, upgrades of existing synchrotrons will result in reducing the size of their x-ray beam – perhaps to sub millimeter - while the beam at HEX is projected to be as large as 25x25 mm. Thus, for large format samples, NSLS II will become unique in the world as an imaging facility.
The high pressure program has an approved Partner User Proposal (PUP) at XPD-D in place, guaranteeing a minimum of 20% of the XPD beamtime for Geosciences oriented high pressure proposals. Additional beamtime can be awarded to competitive General User proposals.

<u>High pressure infrared spectroscopy at FIS</u>

High-pressure spectroscopy provides essential and often unique information about the properties of materials under these conditions. For instance, vibrational infrared (IR) spectroscopy provides detailed information on bonding properties of crystals, glass, and melts, thereby yielding a microscopic description of thermochemical properties. Infrared measurements also provide information on electronic excitations including crystal-field, charge-transfer, excitonic spectra of insulating and semiconducting materials, interband and intraband transitions in metals, and pressure-induced metallization of insulators.
Using synchrotron radiation for infrared studies substantially improves our ability to probe microscopic samples including *in situ* measurements under extreme conditions due to its high brightness, broad-spectrum distribution, and diffraction-limited performance. The development of synchrotron infrared spectroscopy as a whole is fast becoming a leading technique in synchrotron radiation research. The National Synchrotron Light Source (NSLS) has the unique capability to provide synchrotron radiation over a broad range from hard x-ray down to the very far-infrared. The infrared radiation at the VUV ring of the NSLS has world-class performance with up to ~10^4 times the brightness of a conventional thermal (lamp) source. As one of the six infrared beamlines at the NSLS, U2A is the first dedicated high-*P* synchrotron infrared facility in the world, with many unique capabilities compared to high-pressure x-ray beamlines. The beamline was built and managed by Geophysical Laboratory, Carnegie Institution of Washington since 1998 and became available for general users in 2000. The high-pressure infrared program at the NSLS has been very successful in terms of beamline development, outreach of user community, and scientific productivity. A number of important scientific and technical challenges are being addressed at the facility, making it a highly attractive complement to x-ray sources for high-pressure studies. However, NSLS ceased its operation on September 30, 2014.

In order to continue to accommodate the growing user demand and further expand the high-pressure infrared research at the NSLS-II, we proposed the establishment of **F**rontier Synchrotron **I**nfrared **S**pectroscopy Beamline under Extreme Conditions (FIS), an integrated infrared facility dedicated to the study of materials under extreme pressure and temperature (*P-T*) conditions. Through peer review process, our proposal has been approved and NSLS-II is developing the first beamline to extract infrared from one of the special, large-gap dipole bending magnets. These particular magnets avoid cutoff effects that would nominally cause very poor long-wavelength performance, and are arranged in pairs at three locations around the storage ring. Based on the designed storage ring current of 500mA, top-up injection and the overall ultra-high stability of the facility, our performance estimates indicate that NSLS-II will be world-leading in terms of brightness and signal-to-noise over the widest possible spectral range – including the very far-infrared, ideally match the Earth sciences related research under extreme *P-T* conditions.

The current infrared beamline development is part of a larger project called BDN, using the NSLS-II operating funds rather than as a separately funded project. The overall funding is very tight, so only a single extraction is included in this initial infrared beamline development. Two approved beamline programs will share this first IR source at NSLS-II: Frontier Infrared Spectroscopy (FIS) and Magnetic, Ellipsometric & Time-resolved Infrared Spectroscopy (MET). The FIS program will serve the scientific communities studying materials under extreme P-T conditions and is the successor to the very successful U2A beamline at NSLS that has been supported by COMPRES since 2002. The MET program will serve primarily the condensed matter physics and materials science communities for the study of electronic behaviors in solids. Both programs depend on the very high brightness and broadband infrared light produced in the dipole bending magnets of the NSLS-II electron storage ring to achieve diffraction-limited performance in order to overcome the severe throughput limits of diamond anvil cells (DACs), ellipsometers, and inherently small samples. The spectral range includes the very far-infrared which is crucial to study novel behavior such as insulator-metal transitions, superconductivity, ferroelectricity and magnetism, as well as materials ranging from semiconductors and metals, energetic materials, high-explosives, plastics, and complex composites. However, the actual instrumentation used by the FIS and MET science programs are substantially different with FIS using a variety DACs, custom cryostats and a laser system for achieving the extreme sample environments. MET has a high-field magnet and custom spectroscopic ellipsometer as well as plans for a synchronized laser for pump-probe type measurements of dynamical processes. Therefore, FIS and MET plan to share this single extraction by switching the infrared beam between the two sets of endstations. Thus each program will operate 50% of the time. To achieve this, the two sets of beamline endstation instruments will be constructed on adjacent segments of the overall NSLS-II experimental floor space. Another benefit of this space arrangement is that it places the FIS instruments near to the 1st dipole in the same large gap dipole pair (cell 23). Thus, if funding available to build an infrared extraction there, the light could be easily brought to the FIS instruments, providing a dedicated source such that both FIS and MET programs could operate independently at 100% of the time. The estimated cost for building the first extraction and two beamline hutches is ~$2M, covered by the NSLS-II operating funds.

This continued development of synchrotron IR spectroscopy at NSLS-II will provide superior capabilities for in situ studies under extreme conditions in order to address a broad range of scientific issues related to the COMPRES projects in Earth sciences as well as help train next generation scientists. It will not only improve the beamline performance compared to these IR facilities at NSLS but also enable new capabilities including the in situ high pressure and high temperature measurements combining synchrotron IR spectroscopy and laser heating techniques.

Support Laboratory

The build out of a dedicated support laboratory at NSLS-II for the extreme conditions program is paramount for the success of the whole program. We are aware that the space constraints during the ramp up phase of the NSLS-II facility might lead to sharing of laboratory space with other NSLS-II programs on the 1-2 year time scale.

The envisioned laboratory will provide all necessary instrumentation to prepare the sample and the sample environment for an experiment using either the DAC or the MAC. This includes equipment such as a HEPA-filtered fume hood, microscopes, furnaces, electronic-discharge machines (EDM), ball mill, and standard manipulation tools, which serves the basic needs for preparation of pressure cells. Over the initial period 3 year period we envision to extend the capabilities of the preparation laboratory by adding offline laser heating capabilities, laser cutting/drilling capabilities for fabrication of cell parts and a gas loading system for pressure cells.

We envision that the capabilities for sample preparation and manipulation in the support laboratory at NSLS-II will be augmented through a partnership with the Center for Functional Nanomaterials (CFN). The CFN provides a large

number of nano-manipulation and nano-fabrication capabilities that have not yet found their way into the sample preparation or pressure cell development. We plan to exploit the new capabilities to, for example: coat diamonds, allow nano-patterning of samples on the diamond and for recovery of samples after experiments at extreme environmental conditions.

The support laboratory will serve as the nucleation point for an extreme condition research program at many beamlines around the NSLS-II ring.

Establishing Partnerships:

Partnerships are an ideal way to grow the extreme conditions program. *In situ* and *ex situ* experiments on samples at high pressure and temperature as well as samples recovered after exposure to extreme environmental conditions can be conducted on a number of beamlines.

Inelastic X-ray Scattering (IXS) beamline

The inelastic X-ray Scattering (IXS) beamline is one of the six project beamline and is a prime candidate for a partnership with the high pressure program. IXS is one of the beamline that will take full advantage of the unprecedented brightness of the NSLS II beam in the 2-25 keV range.

Experiments at extreme conditions have played a key role in defining the scientific case for IXS and the experimental endstation has been constructed with the needs of high pressure and temperature experiments in mind. IXS will operate in the energy range of 5-15 keV and provide about 1.6×10^{10} photons/s in a 5×7 μm^2 X-ray spot. The beamline enables experiments exploring vibrational dynamics in a broad range of material systems at mesoscopic length scale and picosecond to sub-picosecond time with a world leading sub-meV to 0.1 meV energy resolution (@ 9.1 keV). The spectrometer design provides unique research strengths on liquids, soft condensed matters and bio-molecular systems, as well as powerful performance on the study of relaxation dynamics, sound propagation and transport properties, phonons in crystalline, amorphous and liquid materials, and systems under extreme pressure.

The lead IXS scientist Dr. Yong Cai has an active research program in the investigation of liquids at high pressure and temperature using inelastic X-ray scattering. We already started to explore a partnership between the extreme condition program, mainly focused on the use of diamond anvil cells, at XPD-D and IXS. The experimental capabilities provided by IXS at high pressure and temperature are highly complementary to the diffraction and IR spectroscopy capabilities currently under development at XPD-D and FIS.

Investigations of recovered samples at SRX and TES

The preferable approach to investigate materials structure and properties at extreme conditions are *in situ* experiments that reach the relevant pressure, temperature, stress field, and strain condition of interest. However, the sample environments need to reach extreme conditions limit the techniques that can be used. Especially experiments that probe chemical composition and speciation of a broad range of elements can currently not been conducted *in situ*.

The Submicron Resolution X-ray Spectroscopy beamline (SRX) and the Tender Energy X-ray Absorption Spectroscopy beamline (TES) will enable X-ray fluorescence and measurements on samples recovered from extreme conditions with a sub-micrometer spatial resolution (the current goal is to reach sub-100 nm resolution). The beamlines combined span an energy range from 1-24 keV (SRX: 4.65-25 keV, TES: 1-5 keV) which allows a complete two dimensional characterization of the element distribution in the recovered sample covering the elements from Na to Pd in the periodic table.
Practically all elements relevant in silicate geochemistry are experimentally accessible. For example, the direct determination of the Mg, Al and Si distribution (order-disorder) in a silicate mineral can be determined and local information on the chemical environment can be gained by XAFS measurements.

Partnership with the Center for Functional Nanomaterials

The Center for Functional Nanomaterials at Brookhaven National Laboratory provides the user community with state of the art electron microscopy and sample preparation facilities. The extreme conditions community at synchrotron radiation facilities has not yet fully embraced the Nano-Centers as a resource for sample preparation, machining of parts for environmental cell, manipulation of recovered samples or post experiment characterization.

The CFN provides facilities for a number of mechanical and non-mechanical preparation techniques such as focused ion beam milling, advanced etching and lithography methods for the preparation of TEM samples. These techniques can also be applied to: (*i*) recovered samples as a preparation for further synchrotron experiments e.g. at SRX or TES, (*ii*) sample preparation for a diamond anvil cell experiment, where a specific sample geometry would be beneficial or the sample was part of an aggregate before, and (*iii*) preparation of a recovered sample for investigation using the premier TEM facilities at CFN. BNL has a combined proposal system in place that allows access to NSLS-II and CFN as part of the same general user proposal.

We started a dialogue with CFN leadership to explore a Partnership and access models for extreme environment users of the extreme conditions capabilities at NSLS II beyond the general user system.

In Planning Phase:

The strategic planning workshops at NSLS II in September 2015 will develop the scientific case for the next set of 5-6 beamlines for NSLS II. It is paramount that the extreme conditions user community is actively involved in in these workshops and provides a strong scientific case for extreme conditions research at the new beamlines.

Currently, the most promising development for research at extreme conditions is New York State funded High Energy X-ray beamline (HEX). NY State will invest $25M in the next three years to build a beamline, located at a superconducting wiggler, which provides high energy X-rays to academic and industrial researchers in engineering applications and energy storage.

Although design parameters and management structures are not yet finalized, the X17-program at NSLS, where engineering and high pressure research co-existed so productively, provides a possible template going forward, including the combined use of white and monochromatic beams. It is clear, even at this early stage, that at least in the case of full-field high-energy imaging, HEX will provide an excellent complement to sources, including the NSLS-II micro- and nano-probes, where the concentration is on raster imaging. The proposed key capabilities of the beamline are: (i) three independent beam branches, (ii) white and/or monochromatic beam capabilities in all four hutches, (iii) focusing capabilities for white and monochromatic X-ray beams to a minimum size of $\sim 1 \times 1$ μm^2 with a large working distance using refractive optics, (iv) full field imaging capabilities with a 25×25 mm^2 beam in a variety of imaging modes (absorption contrast, phase contrast, diffraction enhanced etc.), and (v) combined small angle and wide angle scattering capabilities. These experimental capabilities are similar to the needs of the high pressure user community. Therefore, HEX provides a unique opportunity to increase the footprint of the high pressure research program at NSLS-II, without the budgetary burden of building a dedicated high pressure beamline.

The HEX development team and the NSLS II management have invited the high pressure community to participate in the development of the Preliminary Design Report for HEX. We currently have several scientific items under consideration by the NSLS II management.

In the HEX beamline we see the opportunity to increase the breadth of deformation studies to include problems at lower pressures; those relevant to the crust. Presently, with the exception of a few pioneers, the rock mechanics community does not take advantage of the capabilities offered by synchrotron x-rays. With the new diffraction and imaging capabilities envisioned for the HEX beamline we believe that a variety of rock mechanics experiments studying, for example, the evolution of porosity during deformation with and without fluid flow, imaging of faulting in situ, carbon dioxide reactivity with minerals in situ etc will become possible. In order to take full advantage of these capabilities we are starting now to investigate, plan and design new types of sample environments that will enable such experiments. We have formed a small group of Earth scientists to brainstorm about how HEX can be best used by the Earth science community. We expect that this will result in new designs of high pressure equipment that can take full advantage of the HEX beamline.

Reaching Towards Maturity:

In the next phase of development, the goal of the extreme conditions program is two-fold: (i) consolidate the existing user programs and partnerships and (ii) strategically grow the experimental capabilities for research at extreme conditions through partnerships with newly constructed beamlines. The program will include:

- The user programs at the core beamlines XPD and FIS will be fully operational and we will continue to strengthen and develop the user community by adding instrumentation and techniques.
- Expansion of the support laboratory to increase services to more beamlines suitable for extreme conditions experiments and therefore broadening the user community.
- Key will be to instrument HEX for high pressure research, catalyzing technique developments for white beam and large format beams for state of the art imaging.
- Accessing more of CFN and Computational Science Center (CSC), e.g Theory and Computation resources, theory guided and theory aided experiments, e.g. coordination of experiments and theory while the experiment is conducted Engaging new communities e.g. rock mechanics or other near surface research directions

The foundation for the beamline development activities at NSLS II for the next 3-5 years will be laid during the strategic planning workshops in September 2015. We plan to be part of the discussion and promoting the developments that enhance the research capabilities of the COMPRES community.

Note: Further Information on Beamlines

XPD

Lead Scientist: Eric Dooryhee
Beamline Description: https://www.bnl.gov/ps/beamlines/beamline.php?b=XPD-1

FIS

Lead Scientist: Larry Carr, Zhenxian Liu
Beamline Description: https://www.bnl.gov/ps/beamlines/beamline.php?b=FIS

IXS

Lead Scientist: Yong Cai
Beamline Description: https://www.bnl.gov/ps/beamlines/beamline.php?b=IXS

SRX

Lead Scientist: Juergen Thieme
Beamline Description: https://www.bnl.gov/ps/beamlines/beamline.php?b=SRX

CFN – Electron Microscopy

Lead Scientist: Eric Stach
Program Description: http://www0.bnl.gov/cfn/facilities/microscopy.php

HEX

Lead Scientist: Zhong Zhong
Program Description: http://www0.bnl.gov/ps/nsls2/beamlines/map.php

TES

Lead Scientist: Paul Northrup
Beamline Description: https://www.bnl.gov/ps/beamlines/beamline.php?b=TES